DOCKING STUDIES OF CURCUMIN ANALOGS AGAINST METHIONINE AMINOPETIDASE 2 AND BIOLOGICAL EVALUATION OF LEAD MOLECULES IN COLON CELLS

A Thesis Submitted to the
College of Graduate and Postdoctoral Studies
In Partial Fulfillment of the Requirements
For the Degree of Master of Science
In the College of Pharmacy and Nutrition
University of Saskatchewan
Saskatoon

By

Dr. Sukanya Pati

PERMISSION TO USE

In presenting this thesis/dissertation in partial fulfillment of the requirements for a Postgraduate degree from the University of Saskatchewan, I agree that the Libraries of this University may make it freely available for inspection. I further agree that permission for copying of this thesis/dissertation in any manner, in whole or in part, for scholarly purposes may be granted by the professor or professors who supervised my thesis/dissertation work or, in their absence, by the Head of the Department or the Dean of the College in which my thesis work was done. It is understood that any copying or publication or use of this thesis/dissertation or parts thereof for financial gain shall not be allowed without my written permission. It is also understood that due recognition shall be given to me and to the University of Saskatchewan in any scholarly use which may be made of any material in my thesis/dissertation.

Requests for permission to copy or to make other uses of materials in this thesis/dissertation in whole or part should be addressed to:

Head of the College of Pharmacy and Nutrition

107 Wiggins Road

University of Saskatchewan

Saskatoon, Saskatchewan S7N 5E5

Canada

OR

Dean

College of Graduate and Postdoctoral Studies

University of Saskatchewan

116 Thorvaldson Building, 110 Science Place

Saskatoon, Saskatchewan S7N 5C9

Canada

ABSTRACT

Background

Colorectal cancer is one of the major causes of death worldwide. In Canada, colon cancer is the third most commonly diagnosed cancer. Fortunately, 90% of deaths and cases of colon cancer are preventable. If detected at an early stage, it can be cured. There are different challenges in developing a drug for cancer treatments which include tumor selectivity, target specificity, drug efficacy, and overcoming multi-drug resistance (MDR). Designing target specific molecules has brought better success in developing new anticancer agents. Various anticancer targets have been explored for this purpose. Among them, metalloproteinases such as methionine aminopeptidase 2 (MetAP2) play a major role in being an anticancer drug target. This research focuses on the investigation of novel curcumin analogs displaying both MetAP2 inhibitory and cytotoxic properties for further development as anticancer agents.

Purpose

The purpose of this study is to identify promising cytotoxic curcumin analogs as inhibitors of MetAP2 expression and investigate their potential as novel anticancer drug candidates.

Method

The compounds were selected from docking studies against the enzyme MetAP2. They were evaluated for their physicochemical properties through SwissADME scores. The best compounds among the screened compounds were then considered for preclinical evaluations through screening against the colon cancer cell lines HCT116, and HT29, and the normal colon cell line CRL1790 in vitro for their cytotoxic profiles. The best 2 compounds (NC 1768 and NC 1773) were analysed for their inhibitory property against MetAP2 expression in the HT29 cell line using western blot analysis. The Student's t-test for paired data and Dunnett's post hoc test with $p<0.05$ were performed using the program IBM SPSS Statistics 26.

Results

One hundred thirty compounds were docked against MetAP2 enzyme, out of these the top 10 compounds that showed good results for their physicochemical properties assessment were taken for cytotoxic evaluation. Among the 10 compounds, 2 compounds (NC 1768 and NC 1773) had good IC_{50} profiles, and they were analysed using western blot. The western blot indicated that MetAP2 protein expression was reduced by NC 1773 in the HT29 cell line. Dunnett's post hoc test showed significance at $p<0.05$ for the treatment protocol of NC 1773 in comparison with control (cells with absence of treatment). The correlations between the cytotoxicity (IC_{50}) and the physicochemical properties was undertaken using Student's t-test for paired data. The bivariate linear models with logarithmic transformations that were taken for interpretation were linear model, linear-log model, and log-log model. The statistical analysis performed using Student's t-test for paired data was not significant with $p>0.05$ in all 3 bivariate linear models.

Conclusion

The compound NC 1773 has shown excellent results in docking and western blot analysis. It has an ideal IC_{50} profile and predicted bioavailability which warrants further investigation for the mechanism of action.

ACKNOWLEDGEMENTS

I would like to extend my heartfelt and sincere gratitude to Emeritus Professor Jonathan R. Dimmock, College of Pharmacy and Nutrition and Distinguished Professor Rajendra K. Sharma, Department of Pathology and Laboratory Medicine, College of Medicine for their continued support, insightful approach, invaluable guidance, encouragement, and positive environment for research. They have been instrumental in steering the thesis in the right direction, owing to their vast experience in this research area. I am grateful for their trust, constructive comments, patient support, and expertise during my experimental and writing process.

I would like to thank my advisory committee members, Dr. Brian Bandy and Dr. Suresh Tikoo, for providing their invaluable expertise and advice. I am thankful to my graduate chair, Dr. Ekaterina Dadachova, for being a constant guide and motivator throughout my degree.

I would like to express my utmost gratitude to Dr. Umashankar Das and Dr. Swagatika Das. I greatly appreciate your assistance with my research. Thank you for the endless laughter and life advice you have given me. You have taught me so much and I am forever grateful to you.

I express my sincere gratitude to Dr. Meena Sakharkar for her timely advice and skillful guidance. I would like to extend my deep sense of gratitude to my colleagues at Cancer Research Cluster, notably Dr. Ravi Shankar Singh for his prompt suggestions and kindness.

I thankfully acknowledge the College of Pharmacy and Nutrition, and the College of Medicine at the University of Saskatchewan for financially supporting my graduate studies and for giving me the right environment to accomplish my educational endeavors. I duly recognize Maunders McNeil Foundation Inc. for funding this project.

Finally, I would like to wholeheartedly thank my father (Dr. Hari Narayan Pati), my mother (Sujata Pati), my sister (Sukriti Pati), and my loving husband (Jagannath Prasad Dash) for their immeasurable love, support, and encouragement throughout this endeavor. I would like to acknowledge the love and support of my parents, their motivation and faith in me was my greatest strength. A huge thanks to my parents for their sacrifices and reasons beyond number and scope; I would not be where I am without them. Special thanks to my sister, for understanding that this project has cut into our time together, and for continuing to make me laugh and enjoy our moments. I'm particularly grateful for your encouragement dear sister when situations were rough, you have been the pillar to my accomplishments. She has supported and inspired me on this excellent adventure. And a heartfelt thanks to my beloved husband Jagannath Prasad Dash, for his endless love, support, care, optimism, generosity, and patience during my program.

Dr. Sukanya Pati

DEDICATION

This thesis is dedicated to...

...my inspiring father, Dr. Hari Narayan Pati

my caring mother, Sujata Pati

my loving sister, Sukriti Pati

my beloved husband, Jagannath Prasad Dash

and my dear son, Ishaan Dash

TABLE OF CONTENTS

LIST OF TABLES

LIST OF FIGURES

LIST OF ABBREVIATIONS

5-FU	5- fluorouracil
ADME	Absorption, distribution, metabolism, and excretion
BSA	Bovine serum albumin
DMSO	Dimethyl sulfoxide
GI_{50}	Half growth inhibitory concentration
GLIDE	Grid-based Ligand Docking with Energetics
GScore	Glide score
GSH	Glutathione
GST	Glutathione S-transferase
h-MetAP2	Human-MetAP2
IC_{50}	Half maximal inhibitory concentration
IFD	Induced Fit Docking
MDR	Multidrug resistance
MetAP	Methionine aminopeptidase
MetAPs	Methionine aminopeptidases
MMP	Mitochondrial membrane potential
MW	Molecular weight
NFκB	Nuclear factor kappa-light-chain-enhancer of activated B cells
NMT	N-myristolytransferase
PBS	Phosphate Buffer Saline

pp60c-src	Proto-oncogene tyrosine protein kinase
PVDF	Polyvinylidene difluoride membrane
RIPA	Radioimmunoprecipitation assay
ROS	Reactive oxygen species
SDS	Sodium dodecyl sulfate
SRB	Sulforhodamine B
TBS-T	Tris-buffered saline with 0.1% Tween 20
TCA	Trichloroacetic acid
TPSA	Topological polar surface area
vdW	van der Waals
VEGF	Vascular endothelial growth factor
XP	Extra precision

CHAPTER – 1

LITERATURE REVIEW

1.1 Introduction

Colorectal cancer is one of the major causes of death worldwide. In Canada, colon cancer is the third most diagnosed cancer. Fortunately, 90% of deaths and cases of colon cancer are preventable.[1] If detected at an early stage, it can be cured. There are different challenges in developing drugs for cancer treatments, these include tumor selectivity, target specificity, drug efficacy, and overcoming multidrug resistance (MDR). The designing of target-specific molecules has brought better success in developing new anticancer agents. Various anticancer targets have been explored for this purpose; enzymes or biological processes that include tyrosine kinase, metalloproteinases, cyclooxygenases, and antisense oligonucleotides are the major anticancer drug targets. Among them, metalloproteinases such as methionine aminopeptidases (MetAPs) perform a major role in being an anticancer drug target.[2] This proposal mainly focuses on the investigation of novel anticancer molecules targeting MetAPs. Efforts are underway to diagnose cancer at an early stage by understanding molecular mechanisms involved in the genesis of colon cancer and developing new strategies for cancer prevention, early detection, and development of an anticancer drug for treatment.

1.2 Methionine aminopeptidases

Methionine is one of the 20 proteinogenic essential amino acids required for many biological processes such as polyamine synthesis and DNA methylation.[3] Almost all proteins have a common process of amino acid terminal modification for nascent polypeptides occurring inside the cell. Metalloproteinases like methionine aminopeptidase (MetAP) perform the basic function of removal of the essential amino acid methionine from the nascent proteins unblocked N- termini.[4, 5] The maturation of many proteins takes place after the vital step of removal of the N-terminal initiator methionine from nascent polypeptides. This process occurs either co-translationally or post-translationally for the formation of a new protein. The two proposed reaction mechanisms

for MetAP in *E. coli* as depicted in Figure 1.1 are; one, the tetrahedral intermediate is stabilized by Glu204 and the metal center, and second, the tetrahedral intermediate is stabilized by His178 and the metal center.[6] In the mechanisms depicted below E- enzyme, E.S- enzyme+ substrate, E.TS- enzyme+ Transition state of substrate, and S- substrate. This process occurs either co-translationally or post-translationally for the formation of a new protein. In eukaryotes, 80% of proteins go through the removal of the N-termini methionine as an initiation method for the protein translation process. This initiator methionine is responsible for the stability, compartmentalization, and activity of the proteins inside the cell.[3, 7]

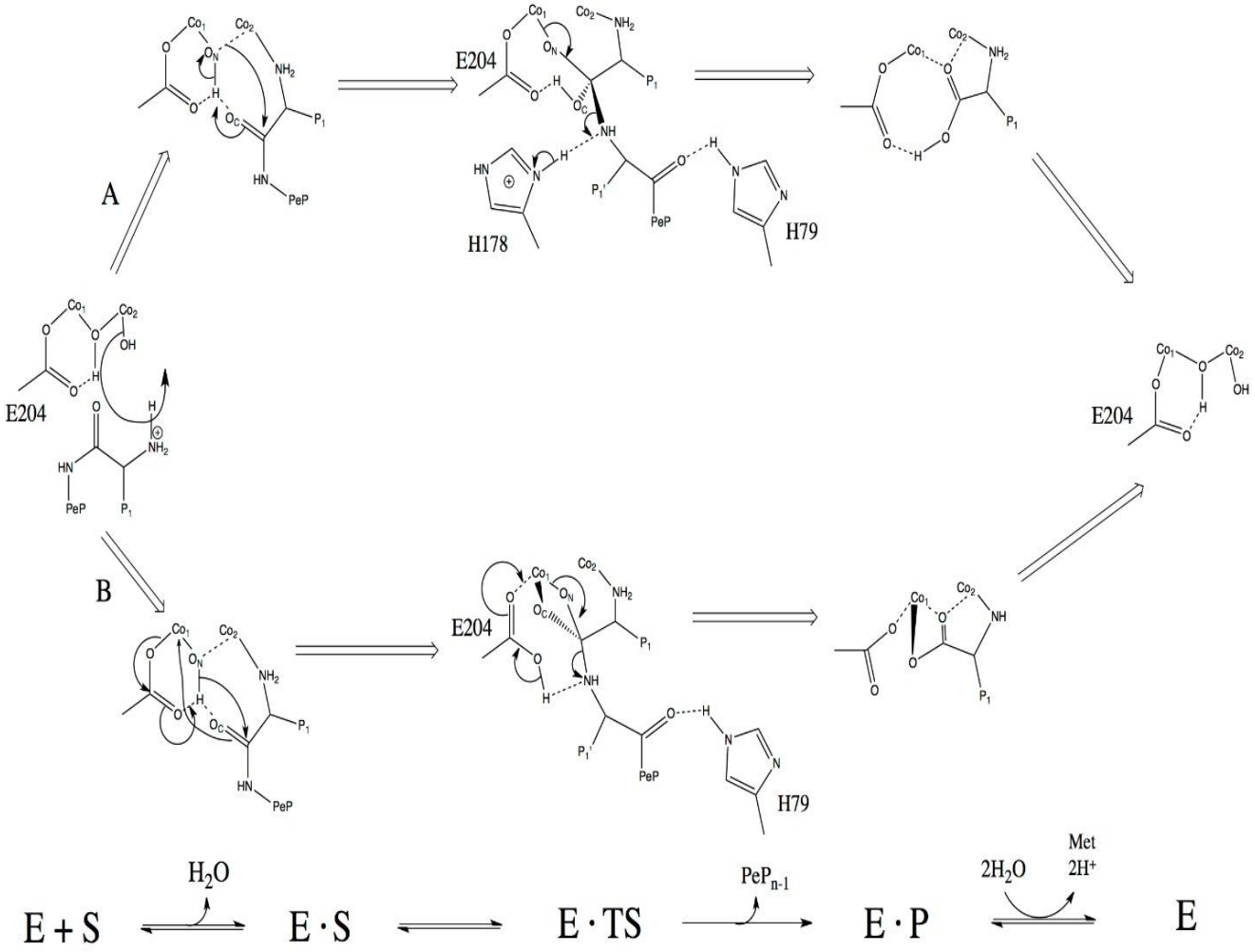

Figure 1.1: Proposed reaction mechanism of MetAP in *E. coli*.[6] In this mechanism E- enzyme, E.S- enzyme+ substrate, E.TS- enzyme+ Transition state of substrate, and S- substrate.

The MetAP exists in two forms that catalyze the methionine cleavage. MetAP1 differs from MetAP2 as it is devoid of a disulfide bond in the crystal structure of the enzyme.[8] This single disulfide bond exists in disulfide (oxidized) and thiol (reduced) states and influences enzyme function thus regulating the enzymatic function of MetAP2.[9] Loss of activity of MetAP2 causes proliferation arrest at G1, whereas inhibition of the activity of MetAP1 leads to cell cycle arrest at G2/M in the mammalian cells.[8]

MetAP co-translationally removes the N-terminal methionine from nascent proteins. This N-terminal methionine is often cleaved when the second residue in the primary sequence is small and uncharged (Met-Ala-, Cys, Gly, Pro, Ser, Thr, or Val). The catalytic activity of human MetAP2 toward Met-Val peptides suggests that it is responsible for the processing of proteins containing N-terminal Met-Val and Met-Thr sequences *in vivo*, as it's consistently two orders of magnitude higher than that of MetAP1.[10]

1.3 MetAP2 and Cancer

Methionine is crucial for tumor cell multiplication and survival.[11-13] Thus, limiting its availability can be a very useful approach to control the proliferation of tumor cells. Since the discovery of the two forms of MetAPs, MetAP2 has been gaining a lot of attention for its role as an anti-angiogenic target in anticancer drug development through expression in cancer cells. It has shown to be overexpressing itself in a variety of cancers.[11, 14] Such an observation was made by our laboratory on MetAP2 in human colorectal cancers. Selvakumar *et. al.* had demonstrated that high expression of MetAP2 in human colorectal cancer contributes to the development of colon cancer.[15] Also, a myristoylated oncoprotein (pp60c-src) is overexpressed along with MetAP2 in tumor cells when compared to normal cells.[15] Selvakumar *et. al.* had demonstrated that MetAP2 and N-myristolytransferase (NMT) genes are upregulated during the malignization of colonic tissues and they have a significant correlation as well.[15] These results were confirmed by enzyme activity, and the MetAP2 expression was significantly higher in Colo320, Colo201, and Colo205 human colon cancer cell lines (HCCLs).[16]

1.4 MetAP2 inhibitors as anticancer agents

Two antiangiogenic compounds, fumagillin, and ovalicin were found to inhibit MetAP2 by binding irreversibly and covalently, leading to cell cycle arrest of endothelial cells at the G1 phase.[17] However there are several other mechanisms by which these compounds may act. For example, fumagillin affects angiogenesis both *in vitro* and *in vivo* by inhibiting the FGR1/ PI3K/ AKT pathways. It has also been shown to inhibit the activity of Bcl-2 and telomerase for metastasis in rats, the growth of hepatocellular carcinoma, and metastasis in mice for the growth of colorectal cancer *in vivo*.[18] In that study, fumagillin increased MetAP2 mRNA expression. *In vitro,* fumagillin was shown to upregulate 71 genes and down-regulate 143 genes along with a significant decrease in the tube formation and proliferation of human umbilical vein endothelial cells (HUVEC).

The removal of the N-terminal initiator methionine from nascent polypeptides is facilitated by the key active site residues and a binuclear metal center in a non-processive manner. The binuclear metal center is bound by monodentate (His-171, Glu-204) and bidentate (Asp-97, Asp-108, Glu-235) ligands, and the nucleophile during catalysis is the metal-bridging water or hydroxide ion. Despite the molecule being overall symmetric, the active site is asymmetrically located with the methionine binding pocket. The binding pocket is primarily generated by residues from the N-terminal domain.[19] Several authors have argued on MetAP2 activity in the presence of iron,[20, 21] cobalt,[21, 22] manganese,[23, 24] and zinc.[24] H178 and H79 are histidine residues that seem to be conserved in all mechanisms mentioned to date, implying their importance in the catalytic activity of MetAP2.[25] X-ray crystallographic data suggest H79 helps position the methionine residue in the active site and transfer a proton to the newly exposed N-terminal amine.[26]

TNP-470, a semi-synthetic analog of fumagillin (Figure 1.2) was found to be 50 times more potent than the parent compound, with an IC_{50} (half maximal inhibitory concentration) of 50 pM being both safe and effective in preclinical trials as well as in several animal models for the treatment of solid tumors.[27] It activates the p53 pathway causing cyclin-dependent kinase inhibition and p21Cip1/Waf1 expression leading to the arrest of progression of endothelial cells at the late G1 phase. It then entered clinical trials in humans for the treatment of AIDS-related Kaposi's sarcoma,

metastatic breast cancer, androgen-independent prostate cancer, pediatric solid tumors, lymphomas, acute leukemia, advanced squamous cell cancer of the cervix, and metastatic renal carcinoma.[28-30] An interactive effect was observed *in vivo* in combination therapy of TNP-470 along with conventional cytotoxic agents.[31-33]

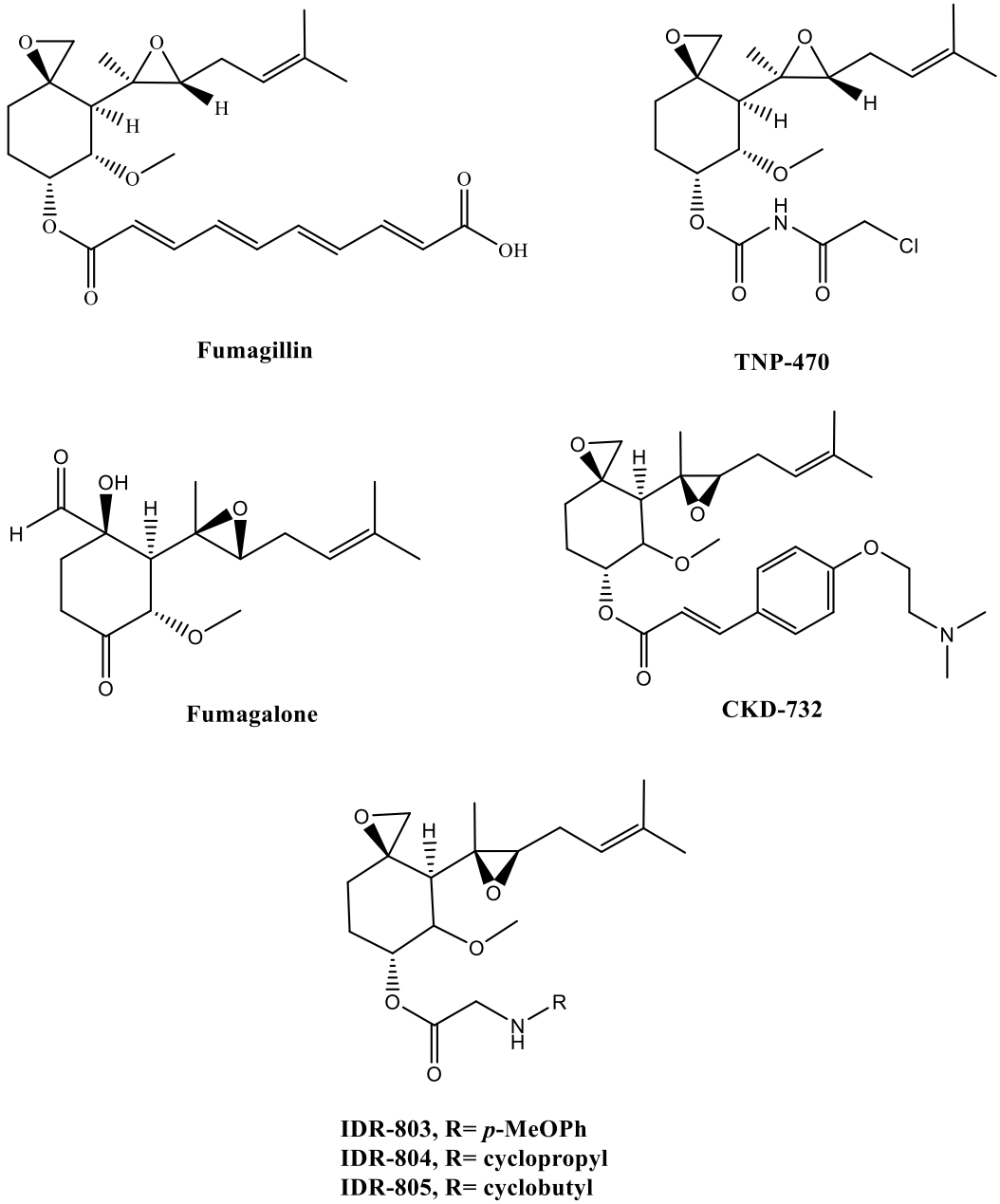

Figure 1.2: Fumagillin and its derivatives demonstrate potent MetAP2 inhibition

Using molecular modeling based on structures, four MetAP2 inhibitors (Figure 1.2) IDR-803, IDR-804, IDR-805, and CKD-732, with high potency were designed and examined against the SNU- 398 hepatoma cell line for their anti-angiogenic effect and capability to inhibit cancer growth *in vivo*.[34] Chun *et. al.* confirmed the ability of these compounds to inhibit cancer growth *in vivo* and identified them as potential anticancer agents.[34]

Fumagalone (Figure 1.2), a synthetic analog of fumagillin has an aldehyde group replacing the spiroepoxide group, which enables it to both inhibit MetAP2 activity and increase the potency by 40 to 50 folds with high specificity towards the enzyme as compared to the parent compound.[35] CKD-732 (Figure 1.2), another semi-synthetic analog of fumagillin, exhibited potency for antiangiogenic activity both *in vitro* as well as *in vivo*. It is 1000 fold more active than the parent compound in inducing cell cycle arrest at G1 and suppressing the proliferation of HUVECs. It is twice better than fumagillin in increasing the life span in nude mice with human tumor PC-3 (prostate adenocarcinoma) and nude mice bearing athymic A375-SM. The potential value of MetAP2 as a novel therapeutic target was greatly accelerated by the development of novel fumagillin analogs with improved pharmacological properties over the parent compound. CKD-732 and TNP-470 (Figure 1.2) have been examined for oncological trials, but their development was terminated because of the adverse events that were a result of their unfavorable pharmacokinetics in the clinical trials.[17] Therefore, the search for new MetAP2 inhibitors as potential cytotoxic agents became essential for the treatment of cancers.

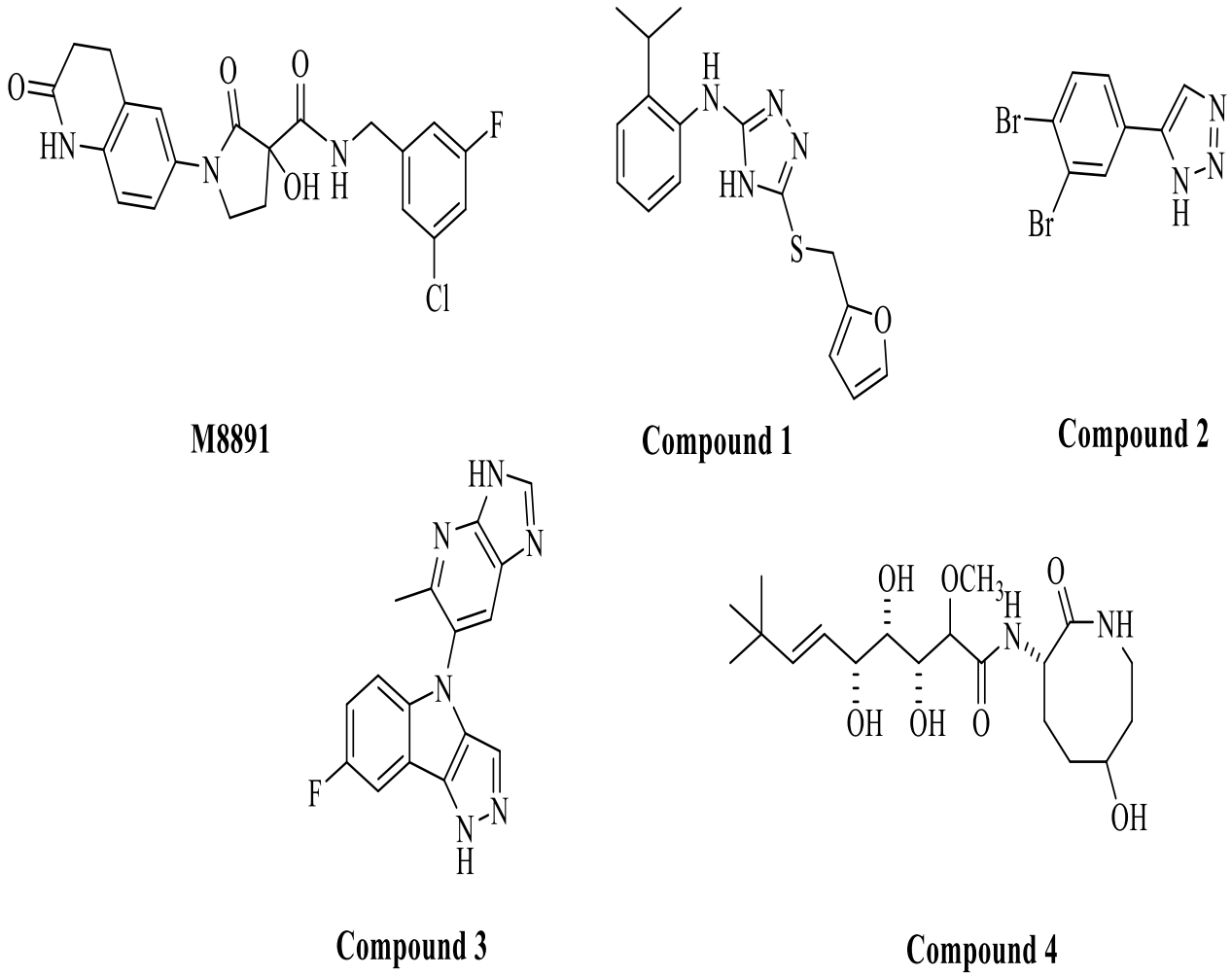

Figure 1.3: Structure of MetAP2 inhibitors

The need for finding structurally divergent MetAP2 inhibitors led to the discovery of several potent lead molecules, compounds **1-4** (Figure 1.3).[36-42] In particular, M8891 was found to be a potent inhibitor of MetAP2 and is currently under phase-I clinical trials.[36] The interaction of M8891 in the MetAP-2 binding site is presented in Figure 1.4. In 1.4A polar interactions are shown to the left and the middle portion depicts the lipophilic contacts the compound is making with the enzyme; all distances are given in angstroms (Å). The right side of the figure has the M8891 surface in green and the molecules are in black while the MetAP-2 pocket is in magenta color (PDB: 6QED). Figure 1.4B at 2Å represents the hydrogen bonds in blue and halogen bonds in

turquoise; the metal interactions are outlined in purple, while the hydrophobic interactions are in grey.

The cyclic tartronic diamide scaffold coordinates in a chelating manner for the two manganese ions. The halogenated benzyl moiety helps in molecular recognition, and it interacts with MetAP2 with van der Waals contacts. The lactam oxygen interacts with the imidazoles of His331 and His339 and Mn2+ ion 508. The amide moiety makes two interactions; one, the amide oxygen coordinates with the buried Mn2+ ion 507, and second, the amide NH interacts with the imidazole of His231. His231 imidazole also makes lipophilic contacts with the tetrahydroquinolinone bound to the lactam nitrogen and the benzylamide residue. The tetrahydroquinolinone residue makes several van der Waals (vdW) interactions at Leu447, His231, Leu328, and a hydrogen bond with Asn329 and the lactam-NH. The fluorine interacts with the side chain of Ala414, while the chlorine interacts with Ile338. Also, the chlorine is involved in a reverse cation−π interaction with the imidazole moiety of His339.

Several MetAP2 inhibitors crystals structures have been published in the last 5 years in RCSB PDB (http://www.rcsb.org/pdb/home/home.do). Among them, 5D6F,[43] 5JFR,[38] 5YKP,[44] 5LYW,[45] 6QEF,[46] and 6QED[36] are some of the noteworthy co-crystals structures with resolutions ranging from 1.5- 1.8 Å. Among the various published co-crystals structures of MetAP2, we have chosen 6QED as the receptor for our research based on its excellent activity and properties. It is a reversible MetAP2 inhibitor with an IC_{50} of 15 nM, it is well-tolerated and has exhibited antitumor efficacy in the mouse glioblastoma model. Figure 1.4C depicts the affinity of M8891 in the receptor pocket at 4Å rendering it to be a good inhibitor of MetAP2. MetAP2 is a monomer containing 365 residues and a total structure weight of 43.37 kDa.

A

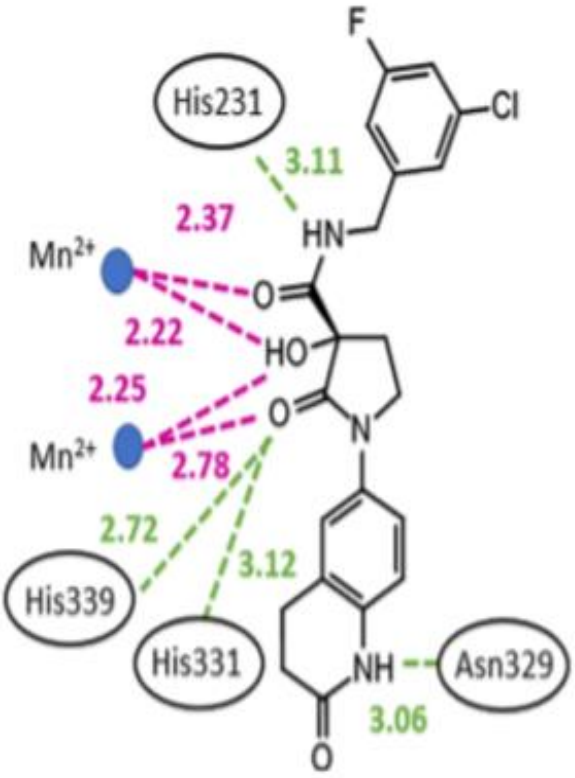
F
Cl
His231
3.11
2.37
HN
Mn2+
O
2.22
HO
2.25
O
N
Mn2+
2.78
2.72
3.12
His339
His331
NH
Asn329
3.06
O

B

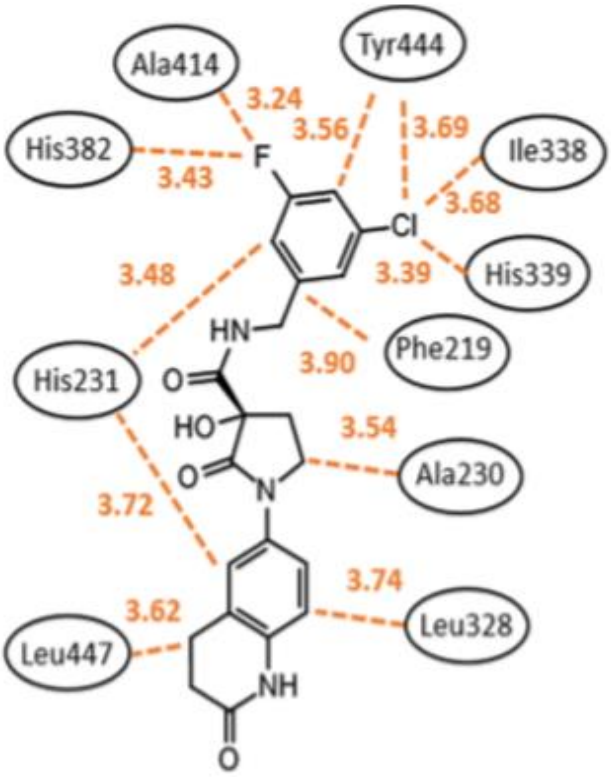
Ala414
Tyr444
3.24
3.56
3.69
His382
F
Ile338
3.43
3.68
Cl
3.48
3.39
His339
HN
3.90
Phe219
His231
O
HO
3.54
O
N
Ala230
3.72
3.74
3.62
Leu328
Leu447
NH
O

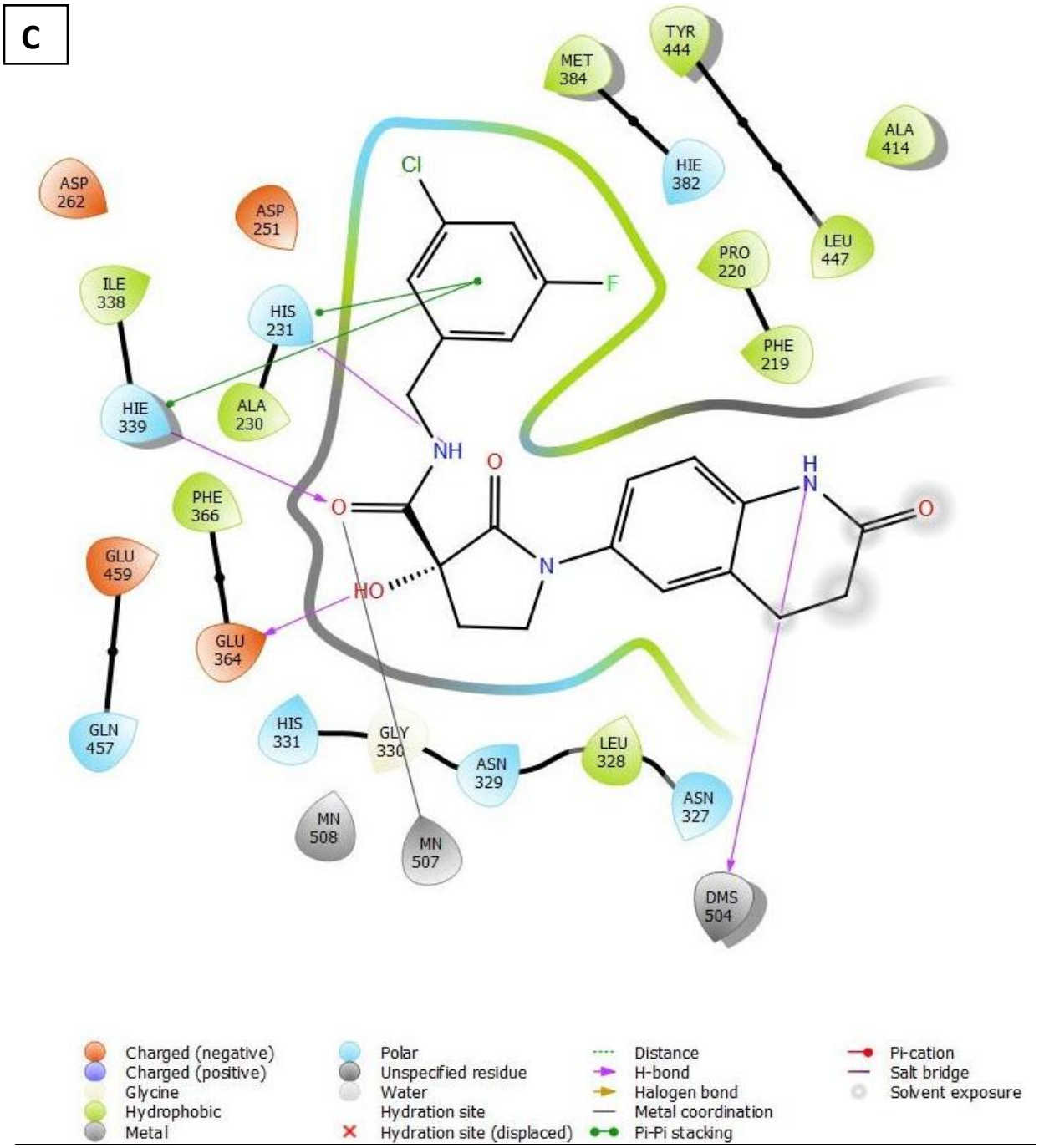

Figure 1.4: M8891 in the active site of MetAP2. 1.4A shows the polar (green) and 4B shows lipophilic (orange) interactions with distances in (Å). 1.4C illustrates M8891 in the binding pocket of the enzyme (PDB:6QED) and its interactions with amino acid residues (π-π stacking-green) and metal ion MN507 (grey)

Target-specific drug discovery has been considered very successful in developing preclinical drug candidates for further drug development. An extensive review of MetAP2 inhibitors was published from Dr. Sharma's laboratory focusing on the involvement of this enzyme in the regulation of various apoptotic factors.[2] Another review by Chiu *et. al.* discussed about the role of disulfide bond of the MetAP2 enzyme that exists in oxidized and reduced states in tumor cells.[9] Stressing the normal cells through oxygen or glucose deprivation results in the enzyme being in an oxidized state. The oxidized and reduced isoforms have different catalytic efficiencies for hydrolysis of MetAP2 peptide substrates. Their findings indicated that MetAP2 is post-translationally regulated by an allosteric disulfide bond, which in turn is responsible for substrate specificity and catalytic efficiency. Continuous efforts have been made to develop structurally divergent new MetAP2 inhibitors to enhance drug specificity and treat drug-resistant colon cancers.

1.5 Curcumin analogs and Cancer

There has been a significant interest in curcumin-based compounds as anticancer agents in the last two decades. Several research studies have been published on the broad biological activities of curcumin which include its anti-inflammatory,[47, 48] anti-oxidant,[49] anti-mutagenic,[49] antimicrobial[50], anti-cystic fibrosis[51], and anticancer[50, 52, 53] properties. However, the clinical potential of curcumin is limited by its extremely low oral bioavailability, due to its chemical instability.[54] In the last two decades, a large number of curcumin analogs have been developed to increase pharmacokinetic properties (Figure 1.5).[55-63] New curcumin analogs have shown improved effects as free radical scavengers[64] and cytotoxic agents.[65] Some also have shown to be potent antitumor agents in MDR cancer cells[66] and also as NF-kB activators.[67]

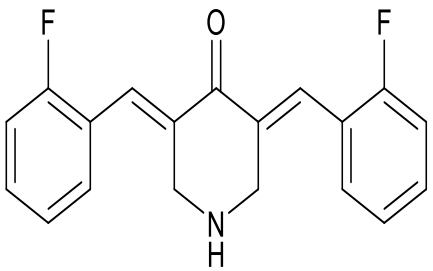

EF 24

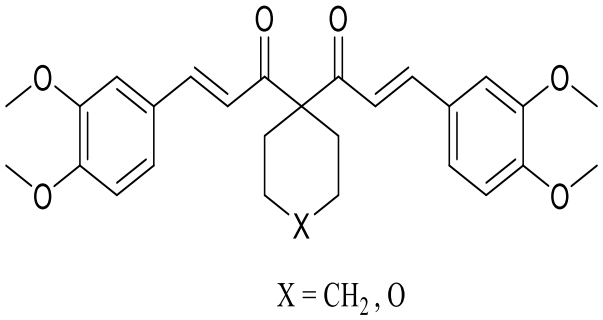

Compound 5a and 5b

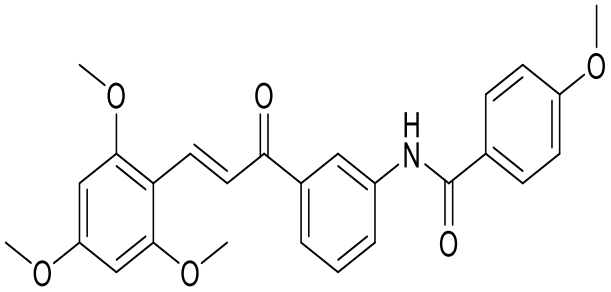

Compound 6

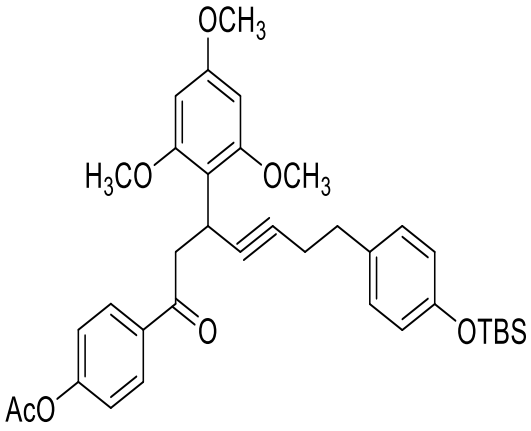

Compound 7

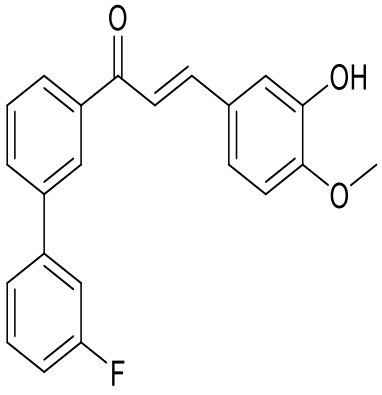

Compound 8

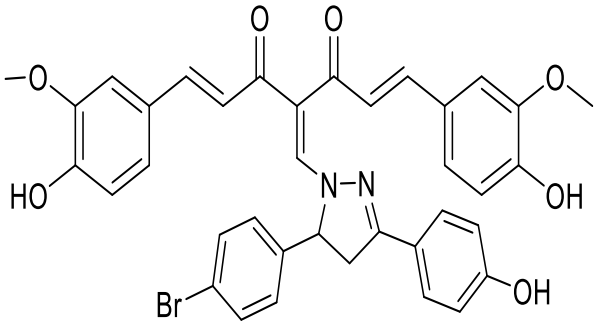

Compound 9

Figure 1.5: Structure of cytotoxic curcumin analogs

EF24, a synthetic analog of curcumin inhibited net cell growth of pancreatic cancer cells with almost 10- to 20-fold lower IC_{50} as compared to curcumin across various cell lines in a concentration-dependent manner. In pancreatic carcinoma (MiaPaCa) and patient-derived pancreatic ductal adenocarcinoma (Pa03C), EF24 annulled the ability of pancreatic cancer cells to form colonies at about 10-fold lower concentrations than curcumin.[55, 56] **5a,** and its more soluble analog, **5b** are structurally distinct curcumin analogs that induced apoptosis in four separate human renal cell carcinoma (RCC) cell lines and human melanoma cell lines. They inhibited *in vitro* generation of myeloid-derived suppressor cells and significantly reduced secretion of vascular endothelial growth factor (VEGF) from RCC cell lines in a dose-dependent manner.[57] Compounds in series **6** had the most potent anticancer activity against renal cell carcinoma (ACHN), pancreatic carcinoma (Panc1), non-small cell lung carcinoma (Calu1), large cell lung carcinoma (H460), and human colorectal carcinoma (HCT116) human cancer cell lines when compared with standard flavopiridol and gemcitabine.[58, 59]

A series of curcumin-based diarylheptanoid analogs **7** have been synthesized and tested for anti-glioblastoma and anti-neuroblastoma effects.[60] At 30 µM, therapy with **7** resulted in the number of colonies declining by 20–25 percent suggesting that the compound-mediated toxicity of hematopoietic cells was not evident *in vitro*.[60] The compound **7** is cytotoxic to the brain and peripheral cancers of the nervous system and has enhanced metabolic and pharmacokinetic profiles.[60] The compound **8**, a novel mono-carbonyl curcumin analog with excellent cytotoxicity against several cancer cell lines. This is also a potent growth inhibitor of human colorectal cancer cells and has been linked with the arrest of cell cycle progression and activation of apoptosis. As a multi-targeted agent, **8** causes cancer cell apoptosis by collapsing the mitochondrial membrane potential (MMP), increasing the Bax/Bcl-2 ratio, then activating the caspase-9/3 cascade.[62, 63] A sequence of Knoevenagel condensates were synthesized with clubbing pyrazole carbaldehydes **9** at the active methylene carbon atom of the curcumin backbone among them **9** was the most active analogue that showed substantial anti-cancer activity against the tested cancer cell line. The proapoptotic activity of compound **9** has been outstanding through the induction of apoptosis in cancer cells. Although the reported effects of cytotoxicity and apoptosis were lower than the standard therapy with paclitaxel.[61]

Many curcumin analogs were designed as thiol alkylators that exert cytotoxicity by alkylation of cellular thiols with the help of the mercapto group present in cellular constituents.[68] They react with glutathione (GSH), metallothioneins, cysteine, and a cysteinyl group of enzymes making it a molecular target. Many α, β-unsaturated ketone compounds (thiol alkylators) were designed by Dimmock and coworkers as cytotoxic alkylating agents based on the principle of sequential cytotoxicity.[69] These α, β-unsaturated ketone compounds have been synthesized with a view to increasing the sensitivity of tumors towards different anti-cancer drugs by reducing the concentration of cellular thiols of tumor cells. The approach of releasing alkylating agents at glutathione-rich tumor sites sequentially is described in the theory of sequential cytotoxicity. As the amount of glutathione S-transferase (GST) may be higher in tumor cells compared to normal cells, α, β-unsaturated ketone compounds are more favorable in decreasing the cellular thiols prior to an attack by an anti-cancer drug.[69] Thus, making the attack more deleterious to tumor cells than normal tissues. α, β-unsaturated ketone compounds as thiol alkylators have been the neoplastic agents that have shown the capability of reversing drug resistance as well.[69]

A series of N-4-(2-aminoethoxy)phenylcarbonyl derivatives of various 3,5-bis(benzylidene)-4-piperidones showed potential cytotoxicity for human leukemia (HL-60), human squamous cell carcinomas (HSC-2, and HSC-4).[70] Among these curcumin-based thiol alkylators, **10** (Figure 1.6) was very specific for human HCT116 colon cancer cells. It had antiproliferative effects by increasing the concentration of reactive oxygen species (ROS), inhibiting the transport chain of electrons, and decreasing the membrane potential of mitochondria. While it exhibited antiproliferative effects for human HCT116 cells, it was less toxic for human non-malignant (CRL1790) colon cells. It induced apoptosis in human HL-60 cells while activating caspase-3 leading to internucleosomal DNA fragmentation and autophagy in human HSC-2 cells.

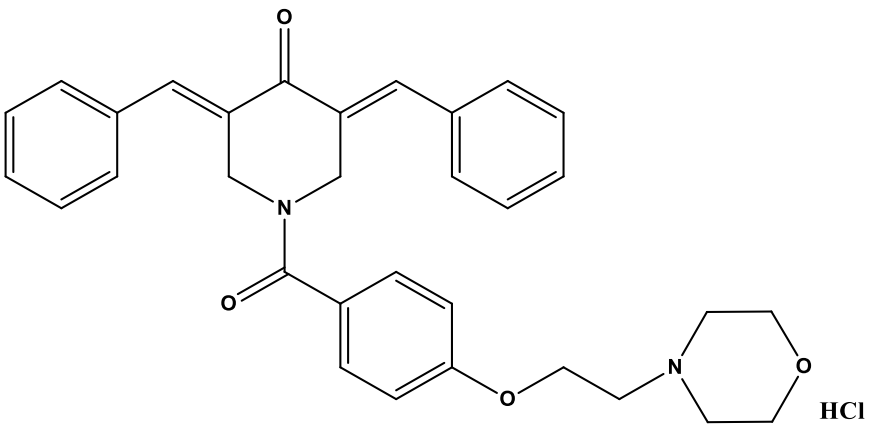

Compound 10

Figure 1.6: Curcumin-based thiol alkylator

Curcumin-derived piperidones have prevailing efficacy in multiple cell lines even at low concentrations. Several (**11a-c:** Figure 1.7) of curcumin-compounds from the three series of novel 3, 5-bis (arylmethylene)-1-(N-arylmaleamoyl)-4-piperidones inhibited proliferation of human Molt 4/C8, lymphoblastic leukemia (CEM) T-lymphocytes, and murine leukemic cells (L1210) as well as exhibiting antioxidant properties as well as topoisomerase IIa inhibitory activity.[71, 72] Curcumin analogs displayed 93-280 folds higher potency in comparison with melphalan. These data suggest the importance of pursuing curcumin analogs as potential cytotoxic agents.

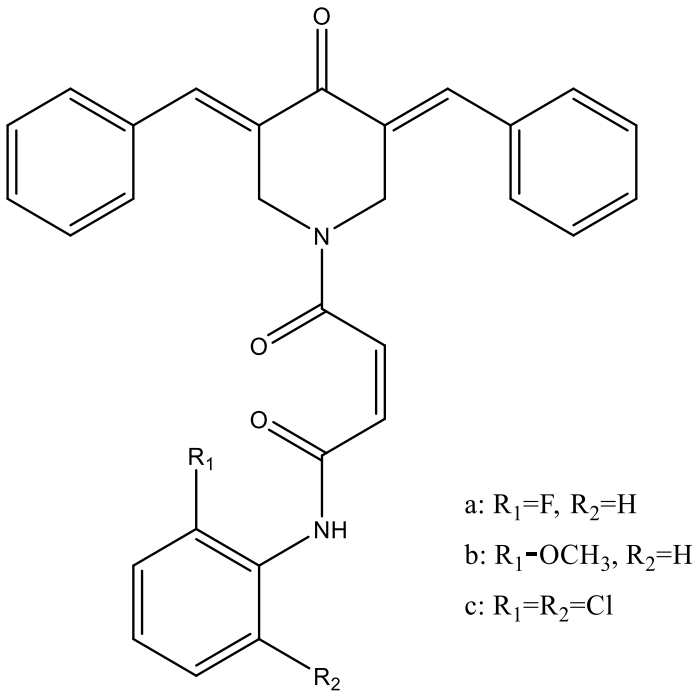

Compound 11

Figure 1.7: 3, 5-Bis (arylmethylene)-1-(N-arylmaleamoyl)-4-piperidones

A recent study by Ocasio-Malavé *et. al.* brought to light the potential of Boc-piperidone chalcones as novel cytotoxic agents against highly metastatic cancer cells.[73] Their ability to induce apoptosis, decrease the activity of nuclear factor kappa-light-chain-enhancer of activated B cells (NFκB), and cellular proliferation is linked to their cytotoxic activity. While compound **6** exhibited equipotent cytotoxicity as cisplatin towards colorectal carcinoma (LoVo) and colon adenocarcinoma (COLO-205) cell lines and less toxicity towards the normal colorectal (CCD18Co) cell lines; compound **12** (Figure 1.8) displayed cytotoxicity towards highly metastatic prostate cancer (PC3 and 22RV1) cell lines by decreasing cell proliferation and the activity of NFκB.

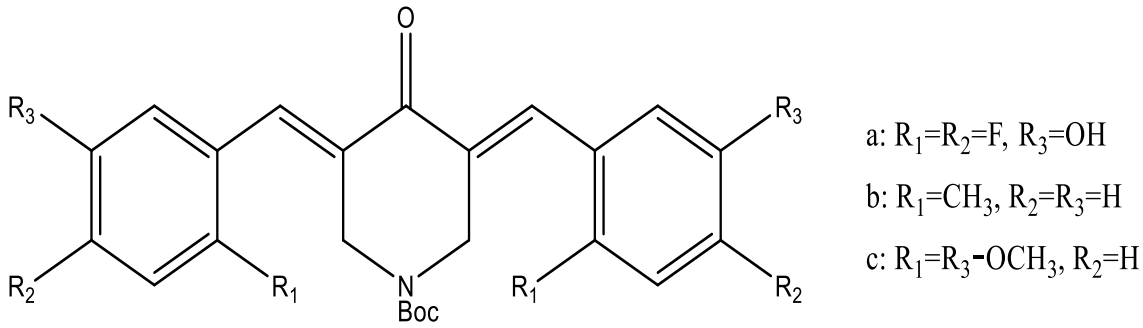

Compound 12

Figure 1.8: 4-Boc-piperidone chalcones

Many of these enones display MDR reverting properties and are well tolerated in a short-term toxicity screen in mice.[74-76] Therefore, the development of novel 3,5-bis-arylidene-4-piperidone derivatives with improved cytotoxic potencies and pharmacokinetic properties may lead to the discovery of a novel drug candidate for treating cancers.

1.6 Curcumin analogs and MetAP2 inhibitors

A wide range of curcumin-related analogs has been developed by Das *et. al.* as anticancer and antiproliferative agents.[77] Several α, β-unsaturated ketones show cytotoxic and anti-cancer properties which interact with cellular thiols, and the conversion of enones increases the rate of thiol alkylation and cytotoxicity. Figure 1.9 delineates a drug design strategy by Pati *et. al.* to undertake structural modification of curcumin to produce novel synthetic analogs as anticancer agents.[78] These enones were designed as thiol alkylators having both cytotoxic properties and the ability to inhibit the MetAP2 enzyme.[79] The dienone pharmacophore is the alkylating active site where thiols can react with the electron-deficient olefinic carbon atoms to cause the inhibition of the enzyme.

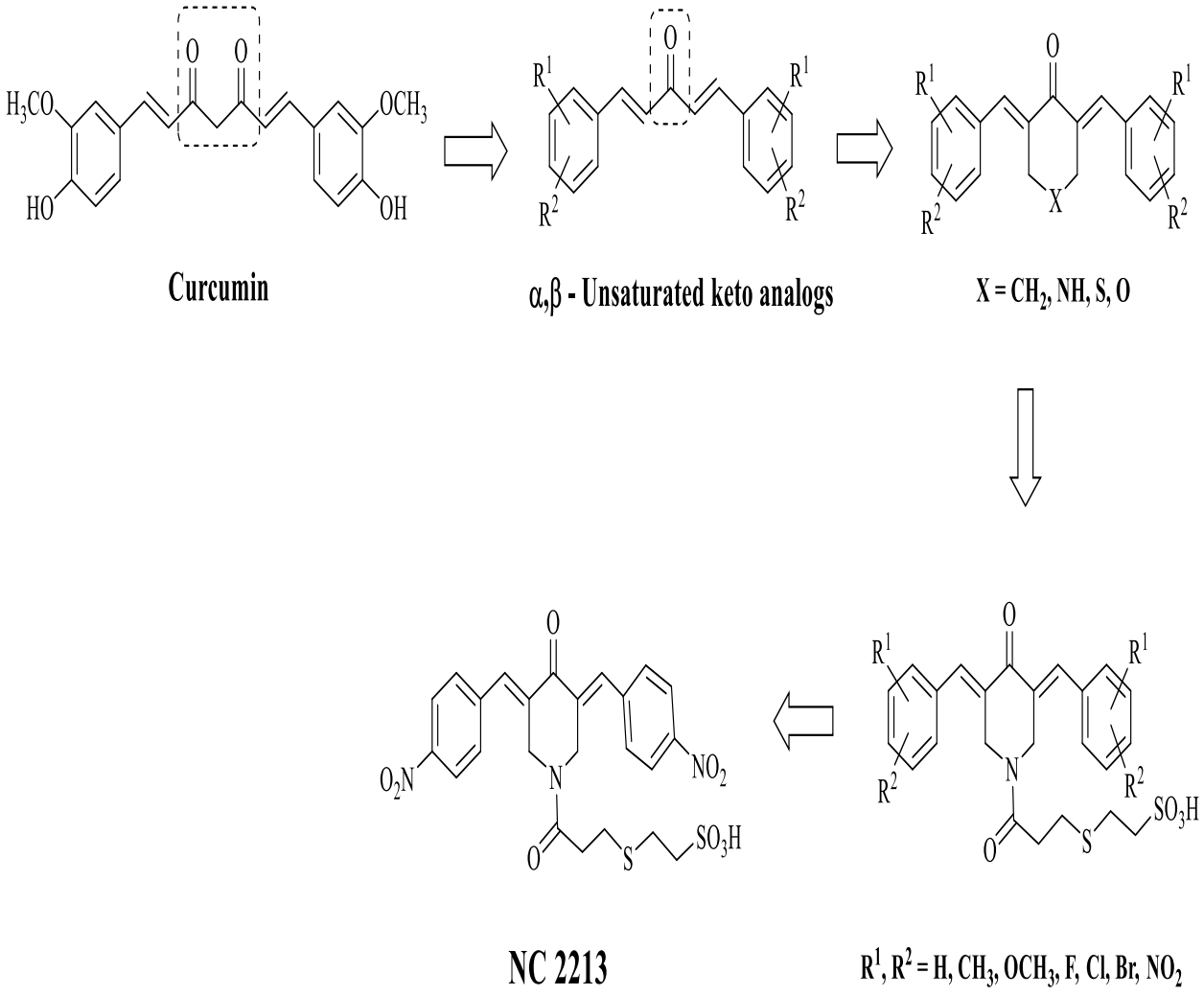

Figure 1.9: Structural modification of curcumin to NC 2213

NC 2213 (Figure 1.9), is a potent cytotoxic agent [IC_{50}: 1.2 µM against human colorectal adenocarcinoma (HT-29) cells] which inhibits Tyr416 phosphorylation of proto-oncogene tyrosine protein kinase (pp60c-src) and activating Tyr527 phosphorylation of pp60c-src at the same time, causing apoptosis of HT29 cells.[78]

CHAPTER – 2

HYPOTHESIS AND OBJECTIVES

2.1 Hypothesis

Cytotoxic curcumin analogs displaying potent inhibition of MetAP2 expression can be developed as therapeutic agents for treating colon cancer.

2.2 Objectives

To identify promising cytotoxic curcumin analogs with the ability to inhibit the MetAP2 protein expression and investigate their potential as novel anticancer drug candidates for treating colon cancers.

To accomplish this objective, the project focuses on the following sub-objectives:

- Literature survey for identifying potent curcumin analogs
- Creation of a database of potent cytotoxic curcumin analogs
- MetAP2-ligand docking studies using the database of curcumin analogs: To identify the best curcumin analogs that show a good fit in the MetAP2 binding pocket.
    - Docking methodology aims to predict the experimental binding modes and affinities of small molecules within the binding site of particular receptor targets and is currently used as a standard computational tool in drug design for lead compound optimization and in virtual screening studies to find novel biologically active molecules. The basic tools of a docking methodology include a search algorithm and an energy scoring function for generating and evaluating ligand poses.[80]

- In silico analysis of the leading compounds from docking studies will be taken for pharmacokinetic and drug-likeness properties

    - Lipinski *et. al.* proposed the "Rule of Five", the most famous drug-likeness filter, which provides four rules to determine whether a molecule is likely to be orally well absorbed or not.[81] When a compound violates two or more rules, it may not be orally active. To be an effective drug, a compound must reach the target in sufficient concentration and be present long enough for the biological effect to take place. It is believed that drugs or drug candidates tend to have similar distributions of physicochemical properties. Hence, based on their respective absorption, distribution, metabolism, and excretion (ADME) properties and drug-likeness it can be determined if a compound is likely to be an efficient drug nominee.

- Cytotoxic and biological evaluation *in vitro*

    - The compounds obtained from the above studies were screened against colon cancer cell lines HCT116 and HT29, *in vitro*. The top 2 compounds were evaluated against non-malignant CRL1790 to identify their selective toxicity to tumors as compared to non-malignant cells. The best 2 compounds (NC 1773 and NC 1768) were analyzed for their inhibitory property against the HT29 cell line using western blot analysis. The physicochemical properties of these compounds were evaluated, and the best compounds satisfying drug-likeness properties, docking well into MetAP2 pocket with good cytotoxicity was considered for further biological evaluations.

- The correlation between cytotoxicity and MetAP2 inhibition of protein expression was investigated using statistical analysis using SPSS software.

CHAPTER – 3

MATERIALS

30% Acrylamide/bis-acrylamide, 37.5:1 (Catalogue#:1610158, Bio-Rad)

5- Fluorouracil (F6627-1G, Sigma-Aldrich)

6 Well cell culture plate (Catalogue#: 14-832-11, Thermo Fischer Scientific)

96 Well cell culture plate (Catalogue#: CS003799, Thermo Fischer Scientific)

Ammonium Persulphate (A3678, Sigma-Aldrich)

Blotting grade blocker non fat dry milk (Catalogue#: 1706404XTU, Bio-Rad)

Bovine serum albumin (PI37525, Thermo Fischer Scientific)

Bradford dye (Catalogue#: 5000205, Bio-Rad)

Clarity Western ECL Substrate (Catalogue#: 17005060, Bio-Rad)

Culture Dish 10mm (Catalogue#: 12-565-91, Thermo Fischer Scientific)

Dimethyl sulfoxide (D8418, Sigma-Aldrich)

EMEM media (Catalogue#: 30-2003, ATCC)

Ethanol (Catalogue#: 001-02-17N)

Fetal bovine serum (Catalogue#: 12483020, Gibco)

Glycine (Catalogue#: BP381-5, Thermo Fischer Scientific)

HRP-linked mouse anti-β-actin antibody (sc-8432, molecular weight- 42 kDa, 1:40,000) (Santa Cruz Biotechnology, Santa Cruz, CA, USA)

McCoy's media (Catalogue#: SH30200.01, Ge Hyclone)

Methanol (Catalogue#: A452-4, Thermo Fischer Scientific)

Penicillin-Streptomycin (Catalogue#: SV30010, Ge Hyclone)

Phosphate Buffer Saline (Catalogue#: SH3025802, Ge Hyclone)

Precision plus protein dual color Standards (Catalogue#: 1610374, Bio-Rad)

Primary antibody: anti-Met-AP2 antibodies (MetAP2 (D3I1H) Rabbit mAb #12547, Cell Signaling Technology)

PVDF membrane (Catalogue#: 1620177, Bio-Rad)

RIPA buffer (R0278, Sigma-Aldrich)

Secondary antibody: Anti-rabbit IgG, HRP-linked antibody #7074, Cell Signaling Technology)

Sodium dodecyl sulfate (Catalogue#:1610302, Bio-Rad)

Sulforhodamine B dye (230162, Sigma-Aldrich)

TEMED (Catalogue#:1610800, Bio-Rad)

Trichloroacetic acid (T9159, Sigma-Aldrich)

Tris base (Catalogue#: BP152-5 Thermo Fischer Scientific)

Trizma base (T1503, Sigma-Aldrich)

Trypsin (Catalogue#: 252000-56, Gibco)

Tween 20 (Catalogue#:1706531, Bio-Rad)

CHAPTER – 4

METHODOLOGY

4.1 Literature survey and database generation

In order to find the potent MetAP2 inhibitors and cytotoxic curcumin analogs from the literature, use was made of SciFinder,[82] PubMed,[83] MEDLINE,[16] and ScienceDirect.[33] Then a library of cytotoxic curcumin analogs was created using Schrodinger.[84] The library constituted of a total of 130 compounds.

4.2 Docking studies

The database of curcumin analogs was docked in the MetAP2 binding site using Schrodinger.[84] This was carried out by complexing the potential curcumin analogs in the h-MetAP2 co-crystal structure 6QED.[36] The curcumin analogs were then ranked according to their docking scores. For this study, the co-crystal structure of h-MetAP2 complexed with M8891 (Figure 1.4) (PDB code: 6QED) was used and the ligand M8891 was removed to dock the compounds in the database. The higher the docking score the better it fits in the MetAP2 active site. The top 10 compounds were taken for biological screening.

4.2.1 The accession of the target protein

The protein of interest is human MetAP2 which is a polypeptide from a unique class of metalloproteases.[5] The removal of the N-terminal initiator methionine from nascent polypeptides is facilitated by the key active site residues and a dinuclear metal center in a non-processive manner. The three-dimension crystal structure of human MetAP2 (PDB: 6QED) in complex with a co-crystallized ligand was retrieved from RCSB PDB (http://www.rcsb.org/pdb/home/home.do).[36]

4.2.2 Molecular docking using Schrödinger

- The protein model was optimized before docking using the Protein Preparation Wizard[85] in Schrödinger Maestro Suite 2014 software (Schrödinger Suite 2014-3 Protein Preparation Wizard; Epik version 2.9, Schrödinger, LLC, New York, NY, 2014; Impact version 6.4, Schrödinger, LLC, New York, NY, 2014; Prime version 3.7, Schrödinger, LLC, New York, NY, 2014). During the optimization process, any inconsistencies in the structure such as missing hydrogen atoms, incorrect bond orders, the orientation of the different functional groups of the amino acids were checked and corrected. The prepared protein was then used for Induced Fit Docking.

- The structures of the compounds were drawn on Maestro (Schrödinger Release 2020-3: Maestro, Schrödinger, LLC, New York, NY, 2020.) and saved as a separate entry to make the database of drugs. These drugs were prepared before docking using the LigPrep application in Schrödinger Maestro Suite 2014 (LigPrep, version 3.1, Schrödinger, LLC, New York, NY, 2014). LigPrep performs optimization of ligand structures viz. conversion of structures from 2 dimensional to 3 dimensional, correction of improper bond distances, bond orders, generation of ionization states, followed by energy minimization. LigPrep generates accurate, energy minimized 3D molecular structures. LigPrep also applies sophisticated rules to correct Lewis structures and to eliminate mistakes in ligands to reduce downstream computational errors. LigPrep optionally expands tautomeric and ionization states, ring conformations, and stereoisomers to produce broad chemical and structural diversity from a single input structure. The ligand structures prepared by LigPrep were used for Induced Fit Docking.

- The Induced Fit Docking (IFD)[86] application in Schrödinger was used to perform flexible protein-ligand docking in our study (Schrödinger Suite 2014-3 Induced Fit Docking protocol; Glide version 6.4, Schrödinger, LLC, New York, NY, 2014; Prime version 3.7, Schrödinger, LLC, New York, NY, 2014). The IFD application in Schrödinger is based on a combination of Grid-based Ligand Docking with Energetics (GLIDE)[84]. The binding site residues are used to generate the receptor grid of the

protein. For the Glide docking stage, extra precision (XP) was selected along with the default cut-off of docking of docked poses within 30 kcal/mol of the best-docked conformation and which are among the top 20 poses. The poses are ranked using Glide score (kcal/mol) and IFD score (kcal/mol). Glide score (GScore) is calculated by the software as

GScore = 0.065*vdW + 0.130*Coul + Lipo + Hbond + Metal + BuryP + RotB + Site,

wherein vdW = Van der Waals energy, Coul = Coulomb energy, Lipo = Lipophilic term, Hbond = Hydrogen-bonding, Metal = Metal-binding term, BuryP = Buried Polar groups' penalty, RotB = Penalty for rotatable bonds that have been frozen, Site = active site polar interactions. IFD score is calculated by the software as IFD Score = 1.0*Glide Score. We have selected the best-ranked conformation of each ligand. The top compounds with Scores (-8.5) and below chosen for their physiochemical properties evaluation.

4.3 Physicochemical properties evaluation

SwissADME[87] was used to predict the drug-likeness nature and the medicinal chemistry friendliness of the compounds. SwissADME web interface is developed and maintained by the Molecular Modeling Group of the Swiss Institute of Bioinformatics (http://www.sib.swiss).[88] It is a free web-based software that was used to predict ADME parameters, compute physicochemical descriptors and pharmacokinetic properties. 2D structural models were drawn directly into the Marvin JS sketcher window and then converted to the SMILES format. SwissADME uses the SMILES format to predict these properties. Based on their respective absorption, distribution, metabolism, and excretion (ADME) properties and drug-likeness were determined if a compound will be an efficient drug nominee. The top 10 compounds that showcased to be efficient drug nominees were taken for their cytotoxic and biological evaluation *in vitro*.

4.4 Cytotoxic studies of the best MetAP2 inhibitors

HCT116, HT29, and non-malignant CRL1790 cells were tested using the sulforhodamine B (SRB) assay in general as described in the literature.[89] The experiments were performed in triplicates.

Five thousand cells were plated per 100 µL (microliter) of McCoy's media at a concentration of 5 x 10^4 cells/mL in each well of a 96-well plate (Plate 1- Tz- control plate, Plate 2- Tc- test plate) and kept in an incubator for 24 hours. After 24 hours, Tz was treated with 25 µL of 50% w/v trichloroacetic acid (TCA) and incubated at 4 °C for 1 hour and then washed with water four times and kept to dry at room temperature. Whereas after 24 hours, Tc was treated with cytotoxic agents. 5- Fluorouracil (5-FU) was taken as a positive control and dimethyl sulfoxide (DMSO) was taken as a negative control. To test the compounds a range of dilutions was prepared in DMSO. The range of dilutions was of five concentrations of positive controls from 100 µM to 0.001 µM using ten-fold serial dilution in 10% (V/V) DMSO and the other 90% is the McCoy's media. 10 µl test sample in 10% (V/V) DMSO was added to each compound well of respective concentrations in the 96-well tissue-culture plate in triplicate. Then 10 µl of 10% (V/V) DMSO was added into each negative-control well and 10 µl 5-FU of 10% (V/V) DMSO was added into each positive-control well. The tests were carried out in triplicates and the different concentrations of the compound were added to the 96 multi-well plates and were left for incubation for 48 hours. After 48 hours, the Tc plate was treated with 50 µL of 50% W/V TCA and incubated at 4 °C for 1 hour and then washed with water four times and left to dry at room temperature. Upon drying 100 µL of SRB solution was added to each well and stained at room temperature for 15 minutes then it was washed with 1% acetic acid about 5 times and kept at room temperature to dry for 24 hours. The cells are washed and stained with SRB solution to monitor the change in adherent cell density. The attached stain was solubilized by adding 200 µL of 10 mM Trizma base solution to each well. The colour absorption was measured after solubilization with Trizma base for 5 minutes on a microplate shaker (room temperature 25 °C, 100 rpm) and the absorbance was measured using a microplate reader at 515 nm. The optical density (OD) of SRB in each well is directly proportional to the cell number and therefore cell growth can be calculated using the formula below:

$$\% \text{ Cytotoxicity} = \frac{\text{O.D.sample} - \text{O.D.control}}{\text{O.D.DMSO} - \text{O.D.control}} \times 100\%$$

The fluorescence values resulting from normalized cell numbers were plotted against the drug concentrations tested to obtain IC_{50} values with GraphPad Prism 8.1.0 software (GraphPad Software, San Diego, CA, USA).

4.5 Cell lysate preparation:

This procedure was performed at 4 °C. Cells after collection were washed twice in Phosphate Buffer Saline (PBS) and lysed in ice-cold , modified radioimmunoprecipitation assay (RIPA) buffer [0.1% sodium dodecyl sulfate (SDS), 1% Nonidet P-40, 0.1% deoxycholate, 0.15 M sodium chloride, 10 mM sodium phosphate (pH 7.0), 100 lM sodium vanadate, 50 mM sodium fluoride, 50 µM leupeptin, 1% aprotinin, 2 mM EDTA, and 1 mM dithiothreitol].[90] Lysates were incubated on ice for 15 minutes and then centrifuged at 14,000 rpm for 5 minutes at 4 °C and the supernatant obtained was used for western blot analysis.

4.6 Western blot analysis of MetAP2 expression

4.6.1 Protein estimation

Protein concentrations were determined by the Bradford method[91] using bovine serum albumin (PI37525, Thermo Fisher Scientific) as a standard.

4.6.2 SDS PAGE

10% SDS- polyacrylamide gel was used to separate the proteins isolated from normal human cells and human colon cancer cells using Laemmli's procedure.[92]

4.6.3 Western blot analysis

MetAP2 expression in colon cancer tissues (HCT116 and HT29) was determined by the immunoblotting method of Towbin *et. al.*[93] Equal quantities of total protein were loaded and separated by 10% SDS-PAGE. The electrophoresed proteins were then blotted onto a polyvinylidene difluoride membrane (PVDF, Catalogue#: 1620177, Bio-Rad), then blocked with 5% w/v non-fat dry milk (Catalogue#: 1706404XTU, Bio-Rad) in Tris-buffered saline with 0.1% Tween 20 (TBS-T). The membranes were incubated overnight at 4 °C with anti-Met-AP2

antibodies (MetAP2 (D3I1H) Rabbit mAb #12547, 1:1000, and molecular weight 63 kDa, Cell Signaling Technology). The samples were washed with TBS-T and then treated with corresponding secondary antibody (Anti-rabbit IgG, HRP-linked antibody #7074, 1:1000, Cell Signaling Technology) for 2 hours at room temperature. Quantification of the western blot bands was performed using the Bio-Rad ChemiDoc imaging system with Clarity™ western ECL substrate (Catalogue #: 1705060, Bio-Rad). Both chemiluminescence (CL) and colorimetric detection methods were used for imaging western blot. The PVDF membrane was then be subjected to a stripping buffer to facilitate accurate detection of the second protein.[94] The membrane was washed with TBS-T and then blocked with 5% w/v non-fat dry milk in TBS-T. It was then treated with HRP-linked mouse anti-β-actin antibody (sc-8432, molecular weight- 42 kDa, 1:40,000, Santa Cruz Biotechnology, Santa Cruz, CA, USA) at room temperature for 1 h. Quantification of the western blot bands was performed using the Bio-rad ChemiDoc imaging system with both chemiluminescence and colorimetric detection methods for imaging western blot.

4.7 Statistical Analysis

Statistical analysis was undertaken to find the correlation between the cytotoxic properties and MetAP2 inhibitors using IBM SPSS Statistics 26 software.[95] Using the program, with variables of HT29 IC_{50}, HCT116 IC_{50}, docking score (aka GScore), molecular weight (MW), LogP, and topological polar surface area (TPSA) the data was evaluated. The bivariate linear models with logarithmic transformations that were taken for interpretation were linear model, linear-log model, and log-log model. The models were used for statistical significance using the Student's t-test for paired data. Dunnett's post hoc test was also performed to compare both the treatment regime of NC 1773 and NC 1768 with control (cells with absence of treatment). A $p<0.05$ was recorded as statistically significant.

CHAPTER – 5

RESULTS AND DISCUSSION

5.1 Database and Docking studies

A literature survey for potent curcumin analogs was completed and the creation of a database of potent cytotoxic curcumin analogs was made. The library of compounds was a total of 130 compounds. An experiment was run using the library of compounds and docked against the MetAP2 binding pocket. The docking scores (aka GScore) were recorded (ranging from -1 to -10). The more negative the docking score the better fit of the compound in the receptor pocket. The docking scores of -8.5 and below were taken for physicochemical properties evaluation.

The docking study targeted PDB: 6QED to examine the potential mode of action of the small compounds as anticancer agents targeting the MetAP2 active site. The ligand-protein interactions were estimated based on the docking score (aka GScore) using the functions implemented in the Induced Fit Docking application in Schrödinger Suite 2014. The docking scores of the top 10 compounds are presented in Table 1. The compound NC 1773 had a docking score of -9.606 while NC 1768 had a docking score of -9.523. All compounds were redocked into active sites in the absence of the reference inhibitor. The ligands were well complexed with active sites of the enzyme.

A recent published study reveals the synthesis and screening of a series of quinoline conjugates for cytotoxic activity using the NCI-60 screen.[96] A single concentration of compound was used. The screening results portrayed that few conjugates were moderately effective against the Renal Cancer cell line UO-31. The data acquired from biological studies was further validated by molecular docking studies (compounds were docked against the active site of the enzyme MetAP-2) and pharmacokinetic evaluation. The docking studies results inferred that the compounds interact with enzyme h-MetAP2 (human-MetAP2) by forming hydrogen bonds in stable conformations as compared to the ligand. Notably, the compounds had same H-bonding interaction with same amino acid HIS231 as that of ligand. The good interaction seen at docking studies was

then validated by the pharmacokinetic evaluation revealing that physiochemical properties were in good agreement with the Lipinski's rule of five.[81]

5.2 Physicochemical properties evaluation

The leading compounds from docking studies were taken for pharmacokinetic and drug-likeness studies. For any bioactive molecule to be considered as a potential drug, it should possess low toxicity with good pharmacokinetic properties. This process was improved based on the high-throughput animal models and while evaluating the toxicity of the drug candidate. The drug likeliness and pharmacokinetic parameters for the compounds were obtained using the SwissADME web interface, developed and maintained by the Molecular Modeling Group of the Swiss Institute of Bioinformatics.

The drug-likeness was evaluated based on the Lipinski rules and the Ghose, Veber, Egan, and Muegge parameters. The more the number of violations the more likely that a compound won't work *in vivo.* The colored zone in the SwissADME column of the table given below is the suitable physicochemical space for oral bioavailability. In this, 6 parameters are taken as prime indicators:

- LIPO (lipophilicity): -0.7 <XLOGP3 <+5.0;
- POLAR (polarity): $20A^2$ <TPSA< $130A^2$;
- INSOLU (insolubility): 0< Log S (ESOL) <6;
- SIZE: 150g/mol <MW <500g/mol;
- INSATU (insaturation): 0.25< Fraction Csp3< 1
- FLEX (flexibility): 0 < # rotatable bonds < 9

Table 5.1: Docking Score and physicochemical properties evaluation

Mol. #	NC #	Docking Score	Structure	SwissADME	MW	TPSA	LogP
1)	1773	-9.606	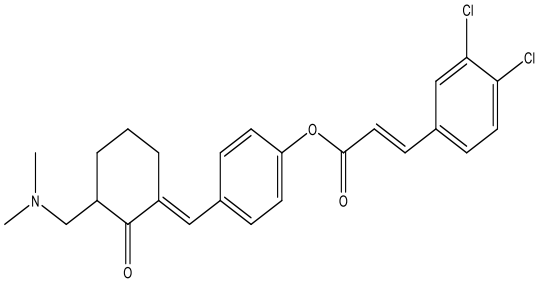	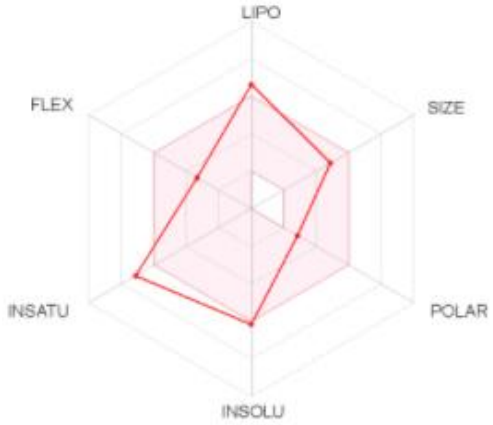	458.38	46.61	5.44
2)	1768	-9.523	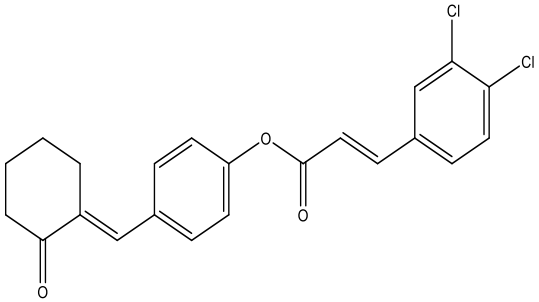	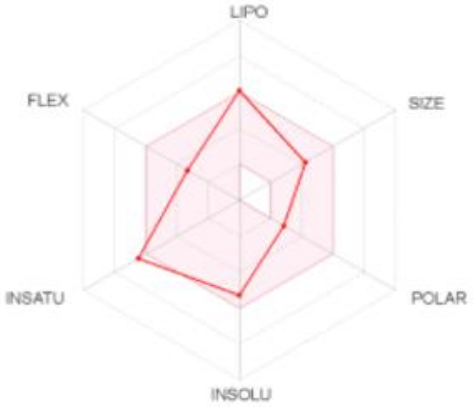	401.28	43.37	5.48

3)	1763	-9.466	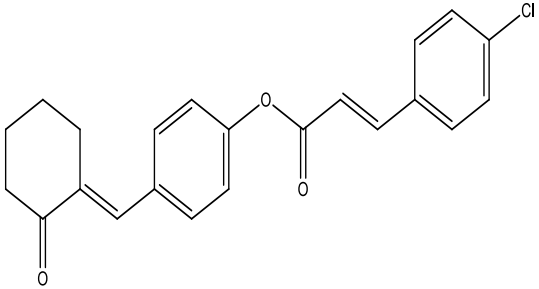	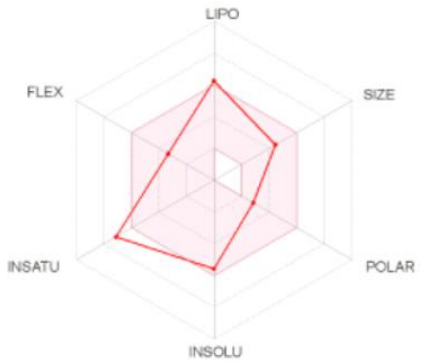	366.84	43.37	4.95
4)	1769	-9.429	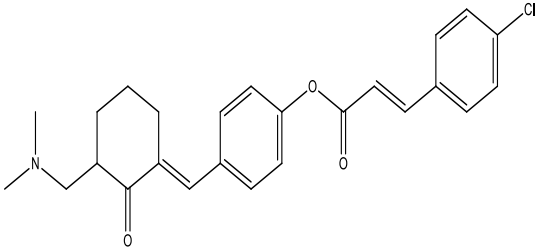	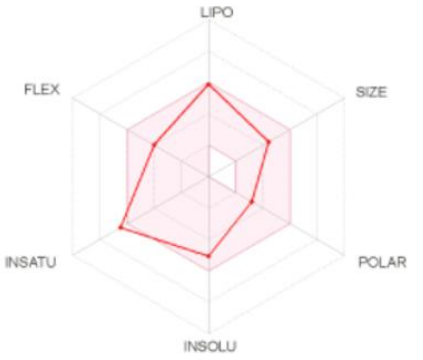	423.93	46.61	4.93
5)	2383	-9.119	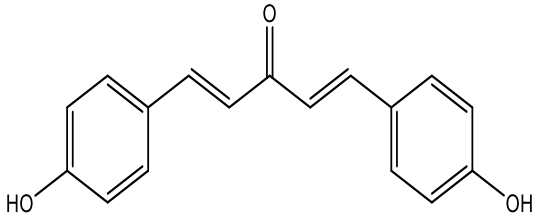		266.29	57.53	3.01

6)	1780	-8.974	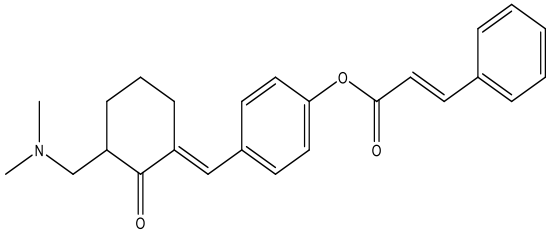	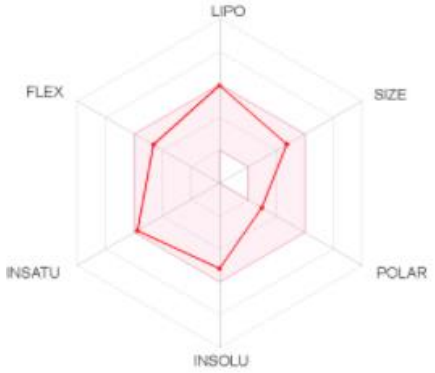	389.49	46.61	4.43
7)	1771	-8.969	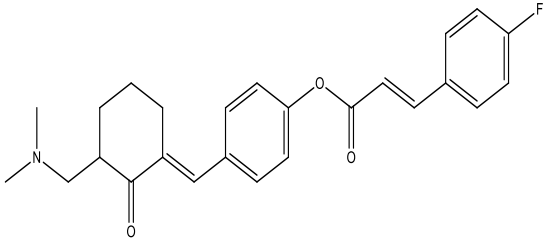	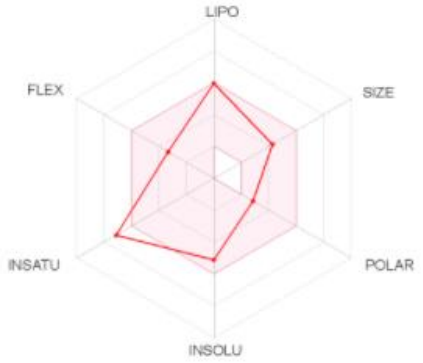	407.48	46.61	4.71
8)	1764	-8.952	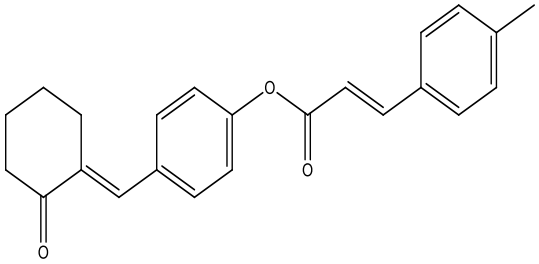	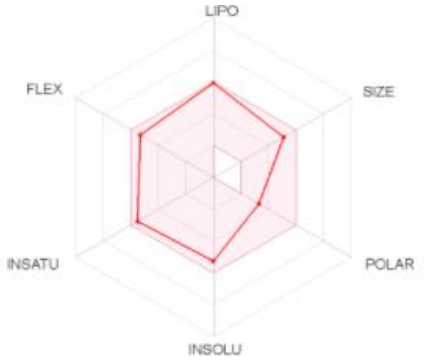	346.42	43.37	4.77

9)	1766	-8.778	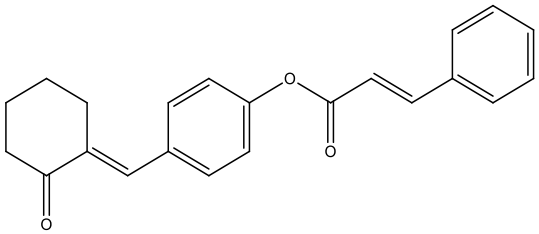	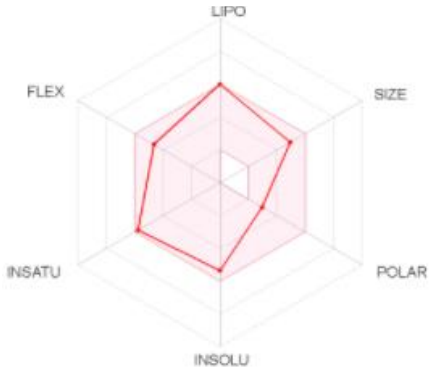	350.38	43.37	4.74
10)	1792	-8.591	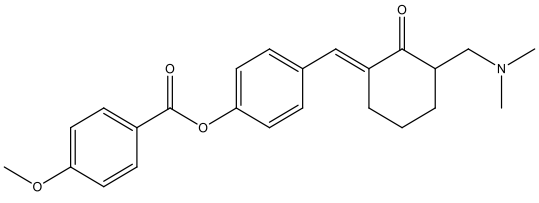	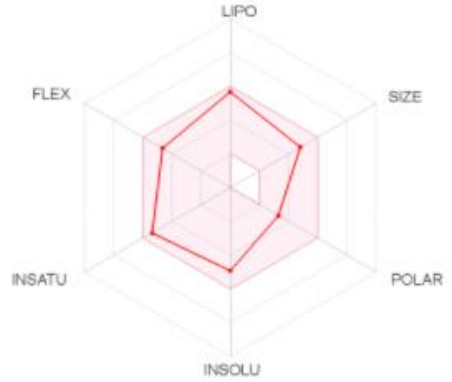	393.48	55.84	4.03

The topological polar surface area (TPSA) is another important pharmacokinetic parameter that predicts the permeability of the membrane by polar atoms.[97] The passive absorption value is $20A^2$ <TPSA< $130A^2$. NC 1773 has a TPSA of 46.61 and NC 1768 has 43.37 as its TPSA. Both the compounds NC 1773 and NC 1768 had a LogP value of 5.44 and 5.48, respectively. Table 5.1 consolidates the most prominent parameters for the compounds to be good candidates for biological evaluation. Based on the above characteristics, we can conclude that the top 10 compounds may have good oral bioavailability as well.

5.3 Biological evaluation

The top 10 compounds that showcased to be efficient drug nominees from the docking studies and their respective physicochemical properties evaluation were taken for their cytotoxic and biological evaluation *in vitro*.

5.3.1 Cytotoxic Studies:

The compounds were tested against HCT116 and HT29 cell lines using sulforhodamine B (SRB) assay. Their respective cytotoxic profiles are given in the Table 5.2 below.

Table 5.2: Cytotoxic profiles of top 10 compounds

Mol. #	NC number	Structure	HT29 IC_{50} in µM (mean± sd)	HCT116 IC_{50} in µM (mean± sd)
1)	1773	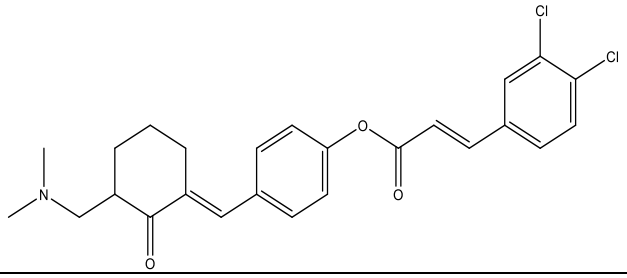	5.51± 0.11	4.21± 0.57
2)	1768	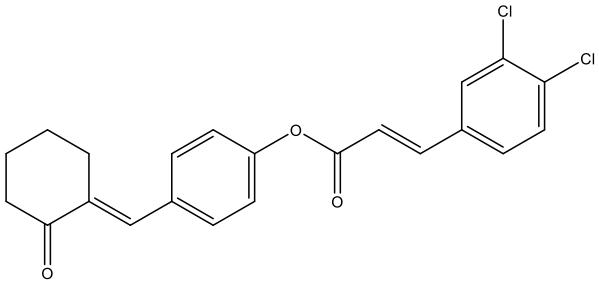	0.24± 0.14	0.57± 0.59
3)	1763	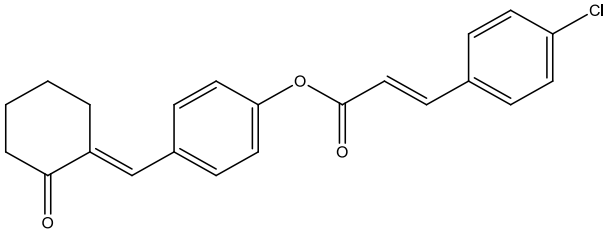	0.54± 0.33	1.02± 0.29
4)	1769	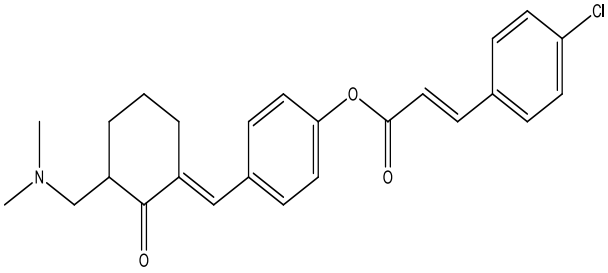	17.63± 1.18	9.21± 0.88
5)	2383	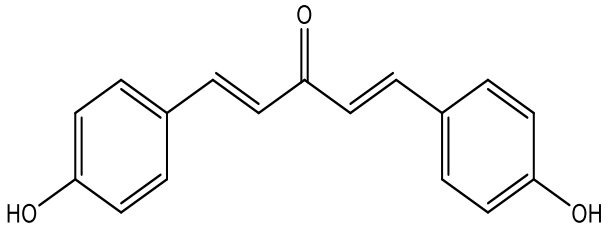	4.79± 0.16	3.57± 0.07

6)	1780	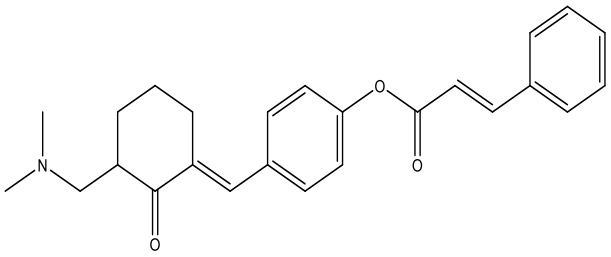	4.99± 1.91	0.19± 0.33
7)	1771	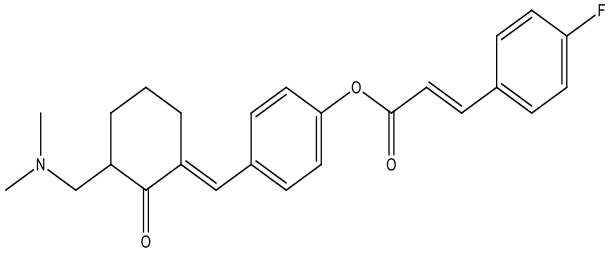	0.32± 0.06	0.15± 0.04
8)	1764	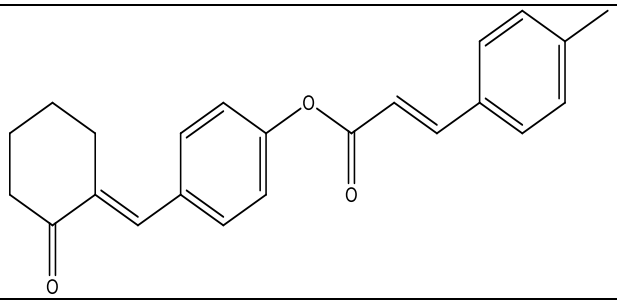	3.95± 0.28	0.05± 0.08
9)	1766	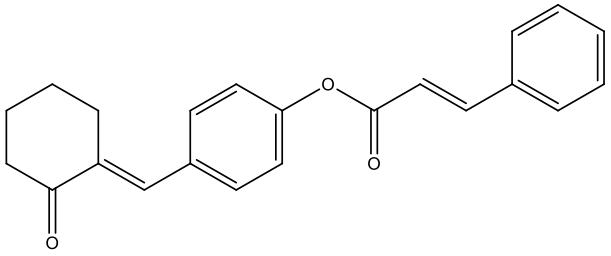	6.06± 0.57	27.90± 0.55
10)	1792	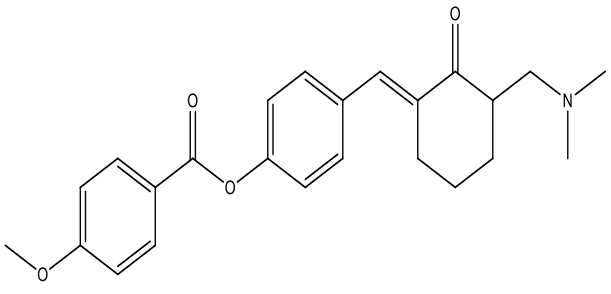	1.12± 0.09	0.37± 0.03

The top 2 compounds from the cytotoxicity studies were taken for screening against the non-malignant CRL1790 cells. A comparison of cytotoxicity for the best 2 compounds was made and it was deduced from Table 5.3 that the compound 1773 is not selective in nature between non-malignant CRL1790 and HT-29 cell line as they have the similar kind of cytotoxic profiles, whereas in HCT-116 cell line it is more cytotoxic and selective than in non-malignant CRL1790 cell line. Compound 1768 is also not selective in nature between non-malignant CRL1790 and HCT-116 cell line as they have the similar kind of cytotoxic profiles, whereas in the HT-29 cell line it is cytotoxic and selective than in non-malignant CRL1790 cell line. All the cytotoxicity results of the studied compounds were compared with the results of the 5FU as the reference drug.

Table 5.3: Comparison of cytotoxicity profiles.

	Cell line	**5FU[b]**	**NC 1773**	**NC 1768**
IC_{50} in µM (mean± sd)[a]	**CRL1790**	14.74± 0.88	4.70± 0.33	0.02± 0.01
	HT29	15.36±0.65	5.51± 0.11	0.24± 0.14
	HCT116	4.02±0.48	4.21± 0.57	0.57± 0.59

a The IC_{50} value in µM (mean± sd) is the concentration of the compound required to inhibit the growth of the cells by 50%.

b 5FU refers to 5-fluorouracil.

Four compounds out of the ten best compounds were previously included in the NCI screening program.[98] The NC Number with their respective NCI numbers are as follows:

a) NC 1773 NCI # 693443

b) NC 1768 NCI # 693441

c) NC 1763 NCI # 693439

d) NC 1780 NCI # 697443

The NCI screening evaluated the compounds against approximately 60 neoplastic cell lines from nine different clusters of cancers namely leukemia and melanoma as well as non-small cell lung, colon, CNS, ovarian, renal, prostate, and breast cancers.[98] The two non-Mannich bases display very weak potency with average GI_{50} (the concentration that causes 50% growth inhibition) values of >96.0 uM (1763, 1768). The average GI_{50} value for melphalan is 19.1 uM and for 5-FU it is 29.5 uM with 3/57 cell lines having GI_{50} values of greater than 251 uM.

On the other hand, the average GI_{50} figures for the Mannich bases 1773 and 1780 are 3.89 uM and 1.98 uM, respectively.[98] In both cases, colon cancer cells and leukemic cells are very sensitive to these two molecules. With these details of bio-evaluations, we can deduce that NC 1773 in comparison to NC 1768 has both desirable IC_{50} and GI_{50} values for it to be a better candidate in being a potent anticancer agent for the treatment of colon cancer.

5.3.2 Western Blot Analysis:

MetAP2 plays a crucial role in the tumor progression of cancer. Previously in a study, MetAP2 mRNA expression was increased by fumagillin.[18] The authors speculated that it may have been an adaptive effect due to inhibition of MetAP2 activity. In our previous study we had demonstrated a high expression of MetAP2 in human colorectal adenocarcinoma and these findings represent the first description of increased MetAP2 expression in colorectal tumors.[79] In addition, with the moderate staining of MetAP2 in polyps exhibited the use of MetAP2 as a novel biomarker for the early detection of colorectal adenocarcinoma using the immunohistochemical approach.[2]

NC 2213, a drug design strategy by Pati *et. al.* was initiated to undertake structural modification of curcumin to produce novel synthetic analogs as anticancer agents.[78] These enones were designed as thiol alkylators. HT29 cells were treated with NC2213 for 48 hours at a concentration range of 0 to 5.0 μM for 96 hours to confirm a dose-dependent inhibitory effect. HT29 cells displayed a significant decrease in MetAP2 expression, this was validated by western blot analysis. Western blot analysis revealed that the MetAP2 expression was inhibited dose-dependently by the treatment of NC2213 using HT29 cells with an IC_{50} value of 1.2 μM.[79] The early investigation of the mode of action of NC 2213 revealed that it is also a potent inhibitor of MetAP2 in HT29 colon cancer cell line.

The best 2 compounds (1773 and 1768) were analyzed for their inhibitory property against MetAP2 protein expression in the HT29 cell line using western blot analysis. The literature survey had already shown that MetAP2 has a higher expression in the HT29 rather than the HCT116 cell lines making it the cell line of choice for the analysis. The results indicated that protein expression was reduced by NC 1773 against the HT29 cell line. The lane with NC 1773 at IC_{50} value showed the maximum reduction of expression while the lanes with NC 1773 at 2 times IC_{50} and ½ of IC_{50} showed about half the reduction in expression of the protein. The lanes with varying concentration of NC 1768 showed no reduction in expression of the MetAP2 protein. The experiment was carried out in technical and biological duplicates. 5-FU and DMSO lanes were taken as standard. The control lane here are untreated HT29 cells. The β-actin served as an internal control. Each lane of an SDS-polyacrylamide gel was loaded with 30 μg of protein. The gel was then immunoblotted

with anti-MetAP2 primary and secondary antibodies for identifying the MetAP2 band. The membrane was then stripped and immunoblotted with an anti-β-actin antibody for identifying the β-actin band as described in "Methodology". The western blot analysis results are shown in Figure 5.1 with the blue marking for the MetAP2 band at 63kDa and the orange marking for the β-actin band at 42kDa.

Figure 5.2 shows the comparison of effects on protein expression between the MetAP2 band and the β-actin band by quantitative analysis of the respective bands using the imaging software from NIH (http://rsb.info.nih.gov/nih-image/download.html). The control lane here are untreated HT29 cells while β-actin served as an internal control. The data presented as the mean (± SE) of at least two separate technical and biological experiments and * depicts the statistical significance ($P < 0.05$) compared to control by Dunnett's Post Hoc analysis.

In Figure 5.4 we can see the histogram depiction of the quantitative analysis of the MetAP2 band (normalized to β-actin) from the western blot analysis. This analysis was carried out with imaging software from NIH. The western blot analysis of extracts from HT29 cells with anti-MetAP2 antibody was carried out with 30µg of protein loaded in each lane of an SDS-polyacrylamide gel and immunoblotted with anti- MetAP2 antibody for imaging the MetAP2 band as described in "Methodology." Dunnett's Post Hoc analysis determined the statistical significance ($P < 0.05$) compared to control. The control lane here are untreated HT29 cells with β-actin as an internal control.

The identification of novel MetAP2 inhibitors in colon cancer cells has provided with new opportunities for preventive or therapeutic interventions by rational drug design. With the details of bio-evaluations, we had deduced that NC 1773 in comparison to NC 1768 had both desirable IC_{50} and GI_{50} values for it to be a better candidate in being a potent anticancer agent for the treatment of colon cancer. In comparison of the IC_{50} values against the non-malignant colon cells, compound 1768 showed to be highly cytotoxic to normal cells making compound 1773 as the compound of choice for further evaluations. Now, with the western blot analysis results, we can

further strengthen the possibility of developing NC 1773 as a MetAP2 specific inhibitor, which may be therapeutically useful.

Figure 5.1: Western blot analysis of effects on MetAP2 expression in HT29. Each lane of

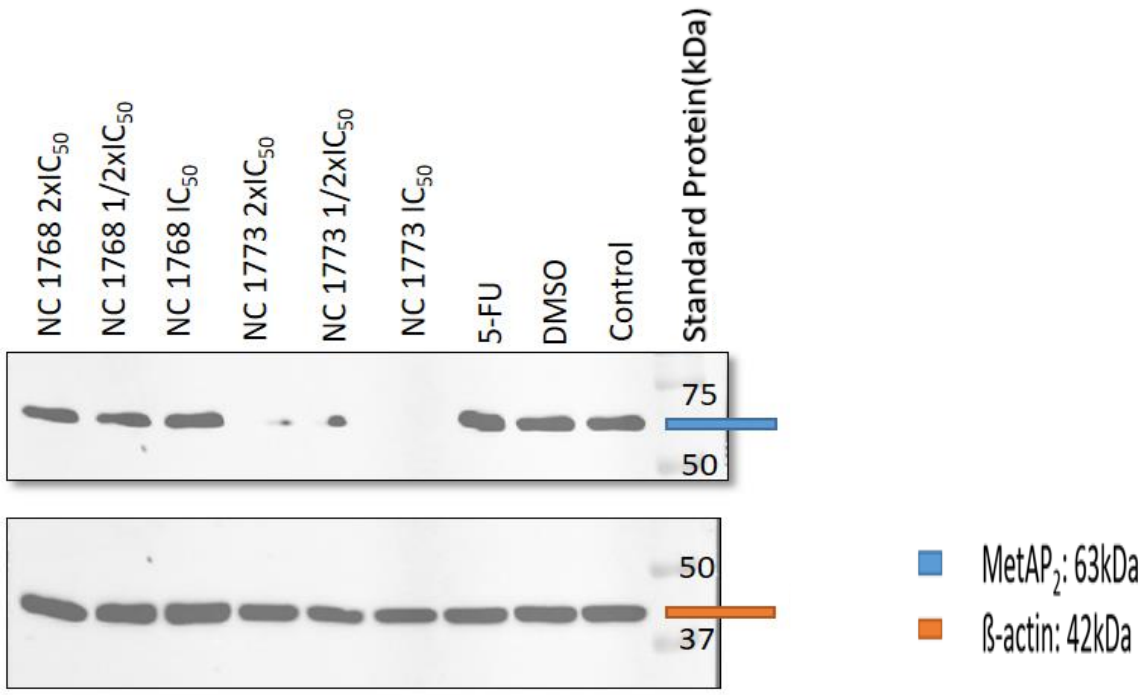

SDS-polyacrylamide gel was loaded with 30 µg of protein. The gel was then immunoblotted with anti-MetAP2 primary and secondary antibodies for imaging the MetAP2 band. The control here are untreated HT29 cells. The β-actin served as an internal control. The analysis was carried out as described in "Methodology". The blue marking is for the MetAP2 band at 63kDa and the orange marking for the β-actin band at 42kDa. The data presented here are representative of at least two separate technical and biological experiments.

Abbreviations: 5-FU stands for 5-flurouracil and DMSO stands for Dimethyl sulfoxide

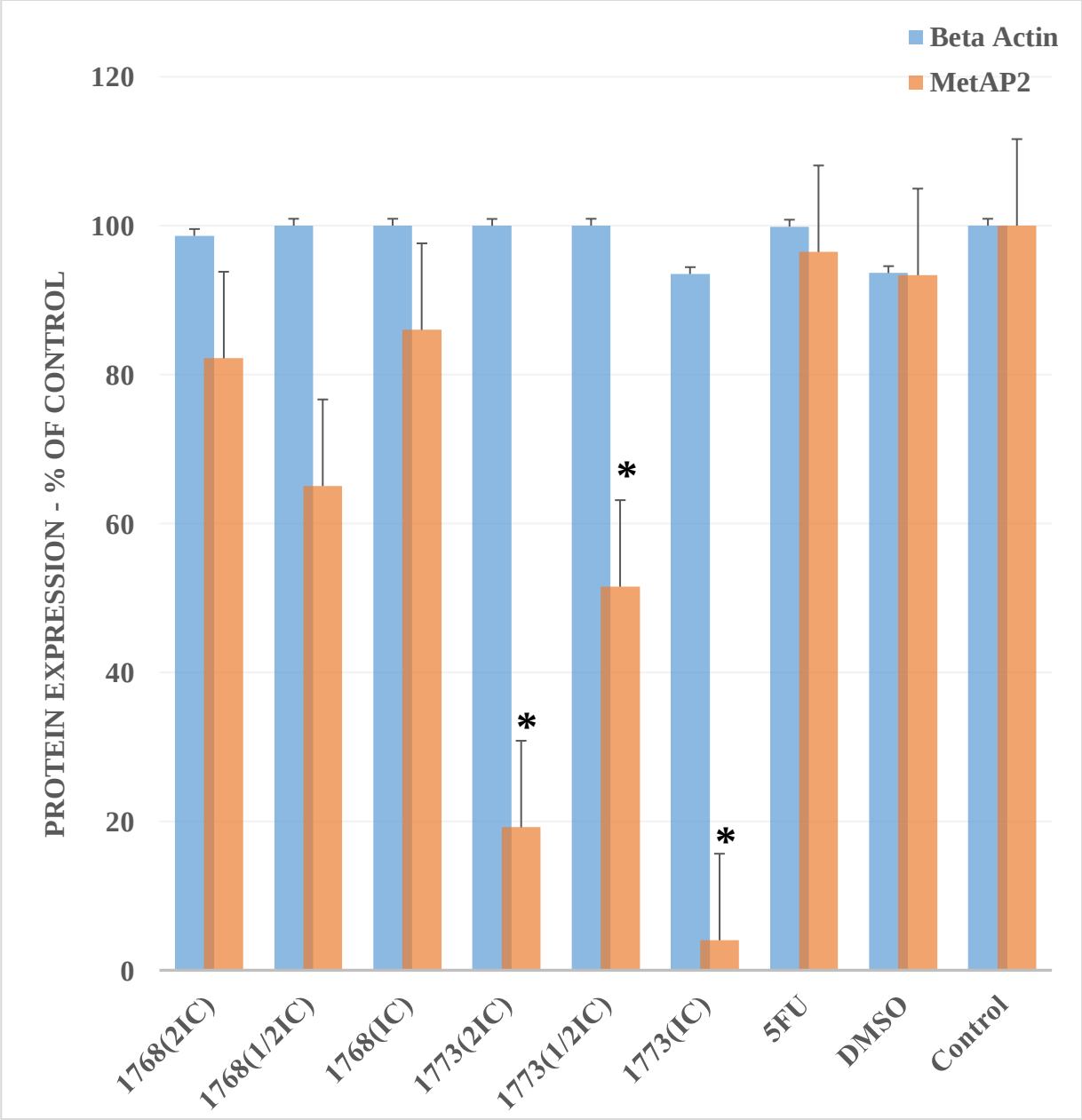

Figure 5.2: Comparison of effects on protein expression. Quantitative analysis of the MetAP2 protein ( ) and β-actin ( ) detected by western blot analysis was carried out with imaging software from NIH (http://rsb.info.nih.gov/nih-image/download.html). The control here are untreated HT29 cells. The β-actin served as an internal control. The data presented as the (mean ± SE) of at least two separate experiments and * depicts the statistical significance ($P < 0.05$) compared to control by Dunnett's analysis.

Abbreviations: 5-FU stands for 5-flurouracil and DMSO stands for Dimethyl sulfoxide

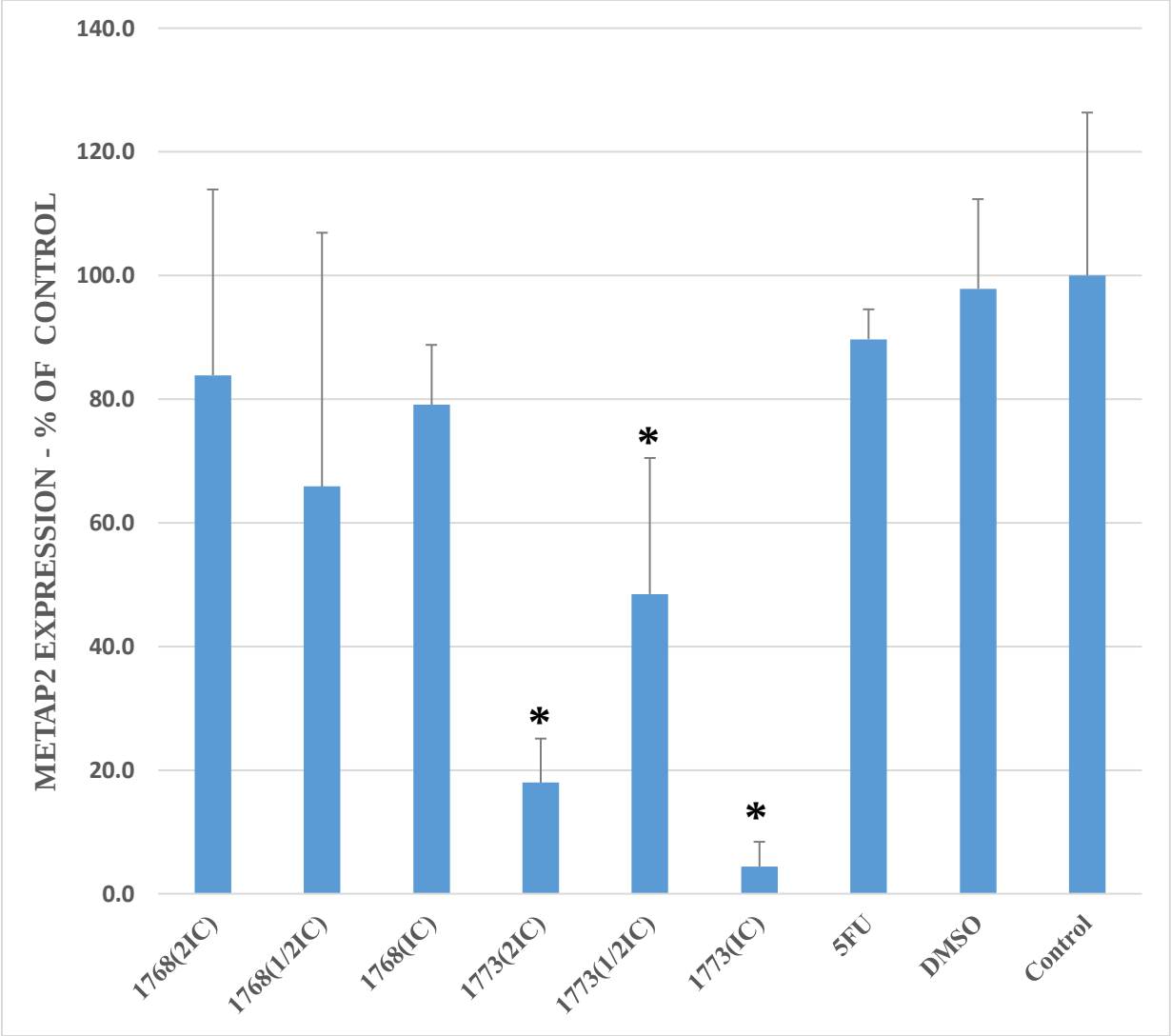

Figure 5.3: Quantification of western blot. Quantitative analysis of the MetAP2 band (normalized to β-actin) was detected by western blot analysis was carried out with imaging software from NIH (http://rsb.info.nih.gov/nih-image/download.html). The data presented as the (mean ± SE) of at least two separate technical and biological experiments and * depicts the statistical significance ($P < 0.05$) compared to control by Dunnett's analysis. The western blot analysis of extracts from HT29 cells with anti-MetAP2 antibody was carried out with 30µg of protein loaded in each lane of an SDS-polyacrylamide gel and immunoblotted with anti- MetAP2 antibody for imaging the MetAP2 band as described in "Methodology."

Abbreviations: 5-FU stands for 5-flurouracil and DMSO stands for Dimethyl sulfoxide

5.4 Ligand Receptor Interaction

The best 2 compounds were screened against the MetAP2 recombinant protein. The MetAP2 protein structure is shown below in Figure 5.4. It is a monomer containing 365 residues and a total structure weight of 43.37 kDa. The docking images for the ligand-receptor interaction were taken at 3 Å rendering it to be a good inhibitor of MetAP2. In Figure 5.5 we can see the interaction of compound 1773 with the receptor pocket. The 2 benzene rings are forming polar interactions with the HIS 231 amino acid residue, and HIE 339 (histidine neutral ε-protonated rotamer). The ketone group is responsible for coordinating with the metal ion both MN507 and MN508, forming the primary binding required for the compound to be bioactive.

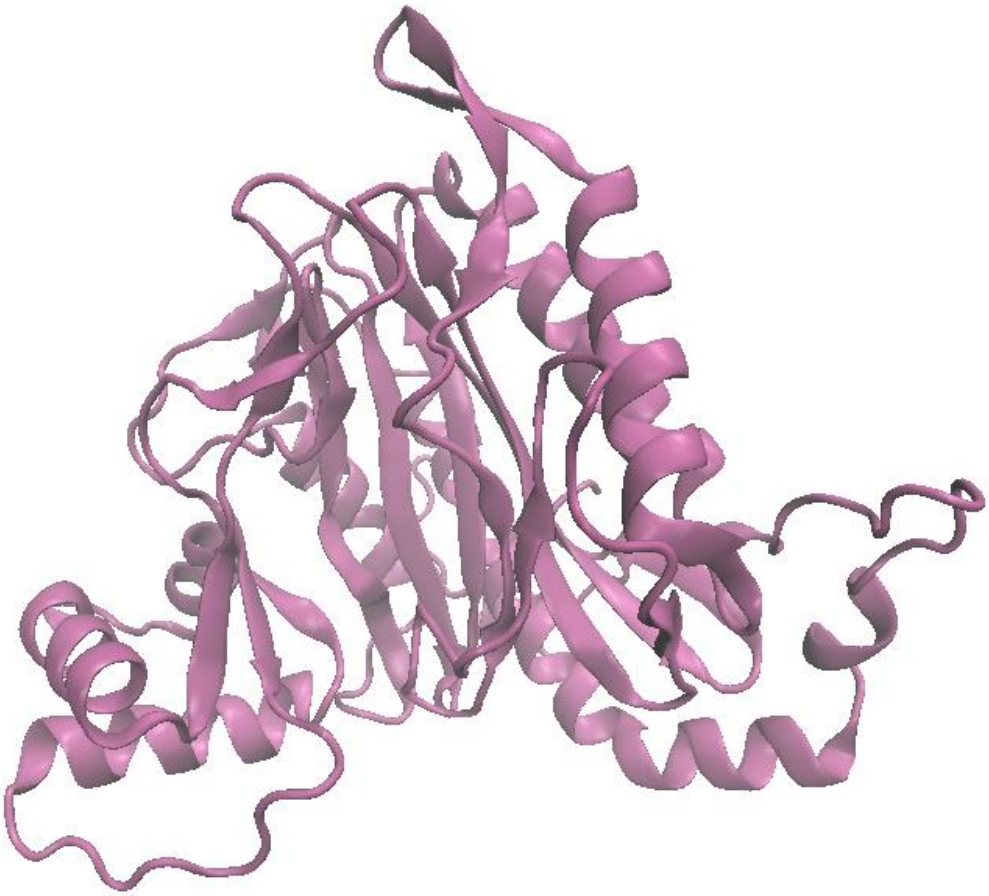

Figure 5.4: Structure of MetAP2 recombinant protein. The enzyme is a monomer containing 365 residues and a total structure weight of 43.37 kDa.

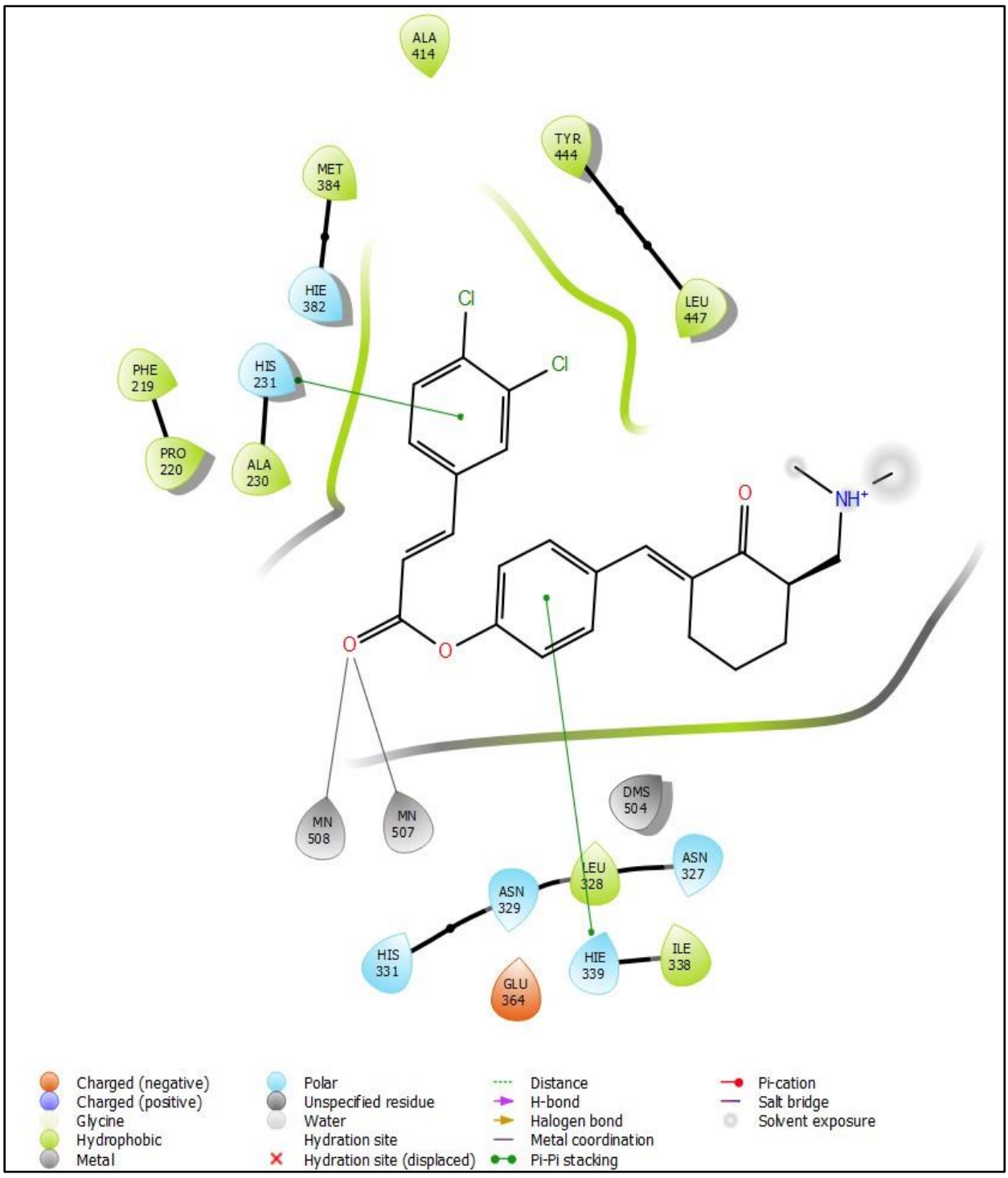

Figure 5.5: Ligand receptor interaction of compound NC 1773. The ketone group is coordinating with both metal ions (grey) and the 2 benzene rings are forming polar interactions (green) with the HIS 231 amino acid residue, and HIE 339 (histidine neutral ε-protonated rotamer).

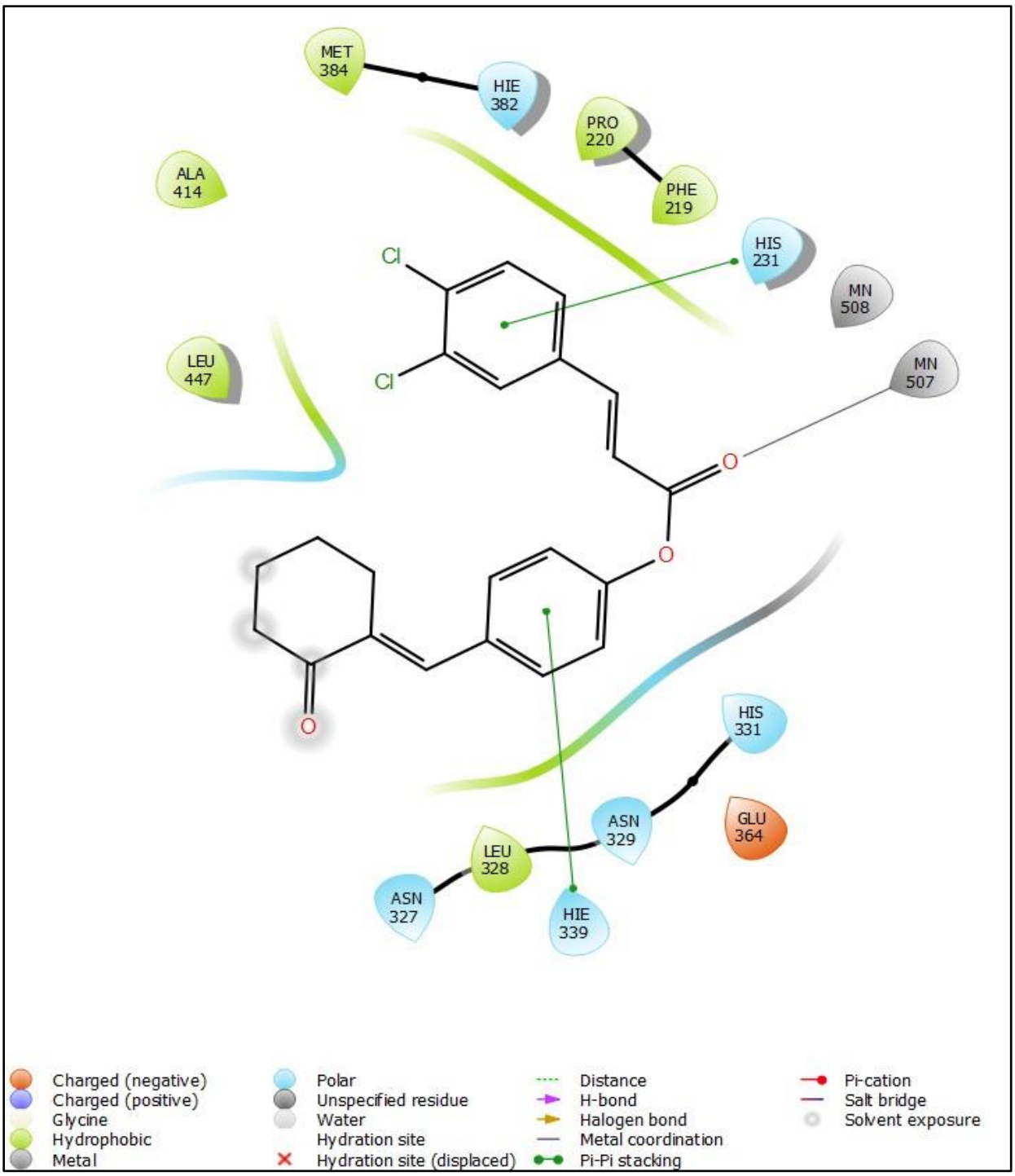

Figure 5.6: Ligand receptor interaction of compound NC 1768. The ketone group is coordinating with MN 507 (grey) and the 2 benzene rings are forming Pi-Pi stacking interactions (green) with the HIS 231 amino acid residue, and HIE 339 (histidine neutral ε-protonated rotamer).

From Figure 5.6 we can see the interaction of compound 1768 with the receptor pocket. The 2 benzene rings are forming polar interactions with the HIS 231 amino acid residue, and HIE 339. The ketone group is responsible for coordinating with the metal ion MN507, forming the primary binding required for the compound to be bioactive. While the interaction with the amino residues is the same for both the compounds, the ability of compound 1773 to coordinate with 2 metal ions contributes it to be more bioactive than 1768 and this is well depicted in the biological evaluations as well.

In Figures 5.7 and 5.8, the visual representations of the compounds 1773 and 1768 docked into the binding pocket show that both the compounds have very good docking in the receptor pocket with good amino acid residue interactions and coordination with the metal ions. In figure 5.8 there is a special indication of the amino acid residues and the metal ions proposed to be vital in the interaction and bioactivity of the compounds.

NC 1773

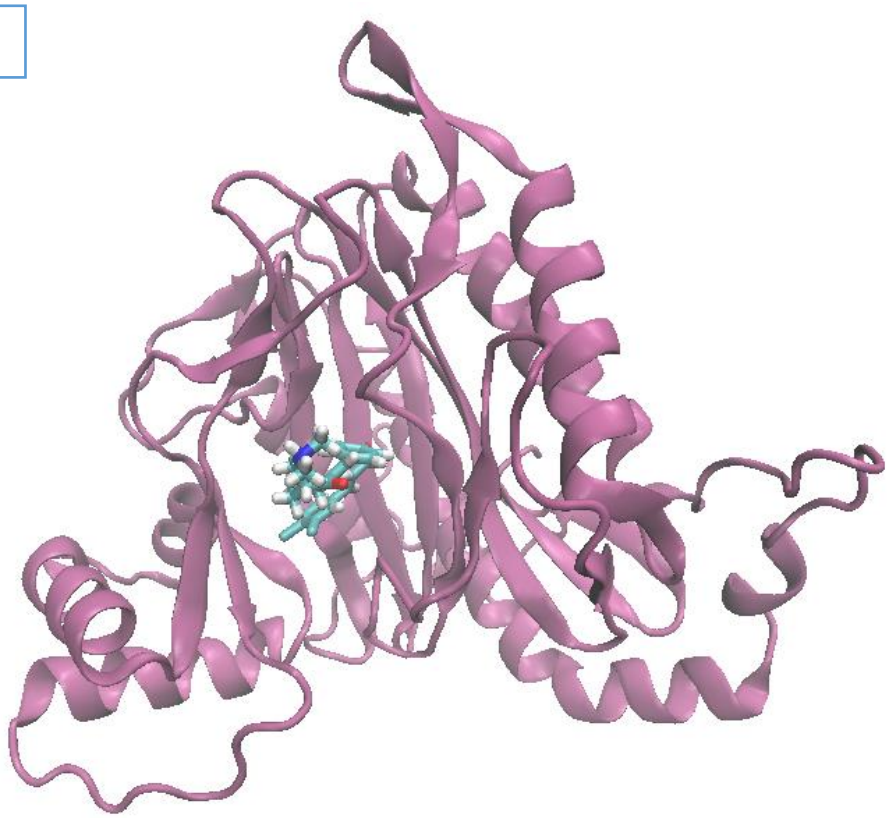

NC 1768

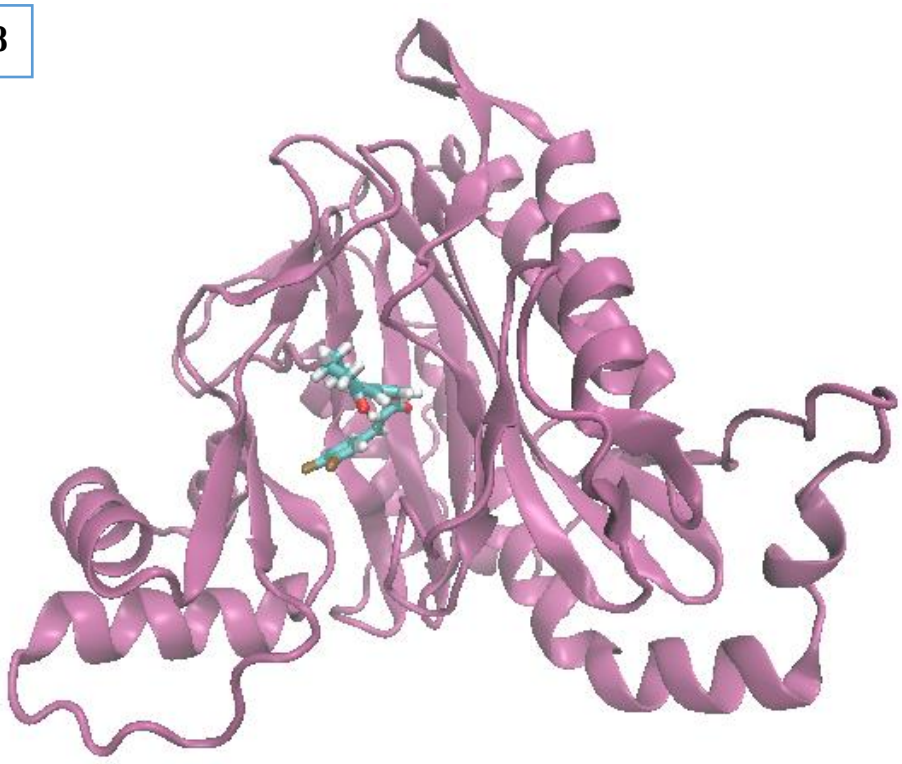

Figure 5.7: Visual representations of the compounds NC 1773 and NC 1768

NC 1773

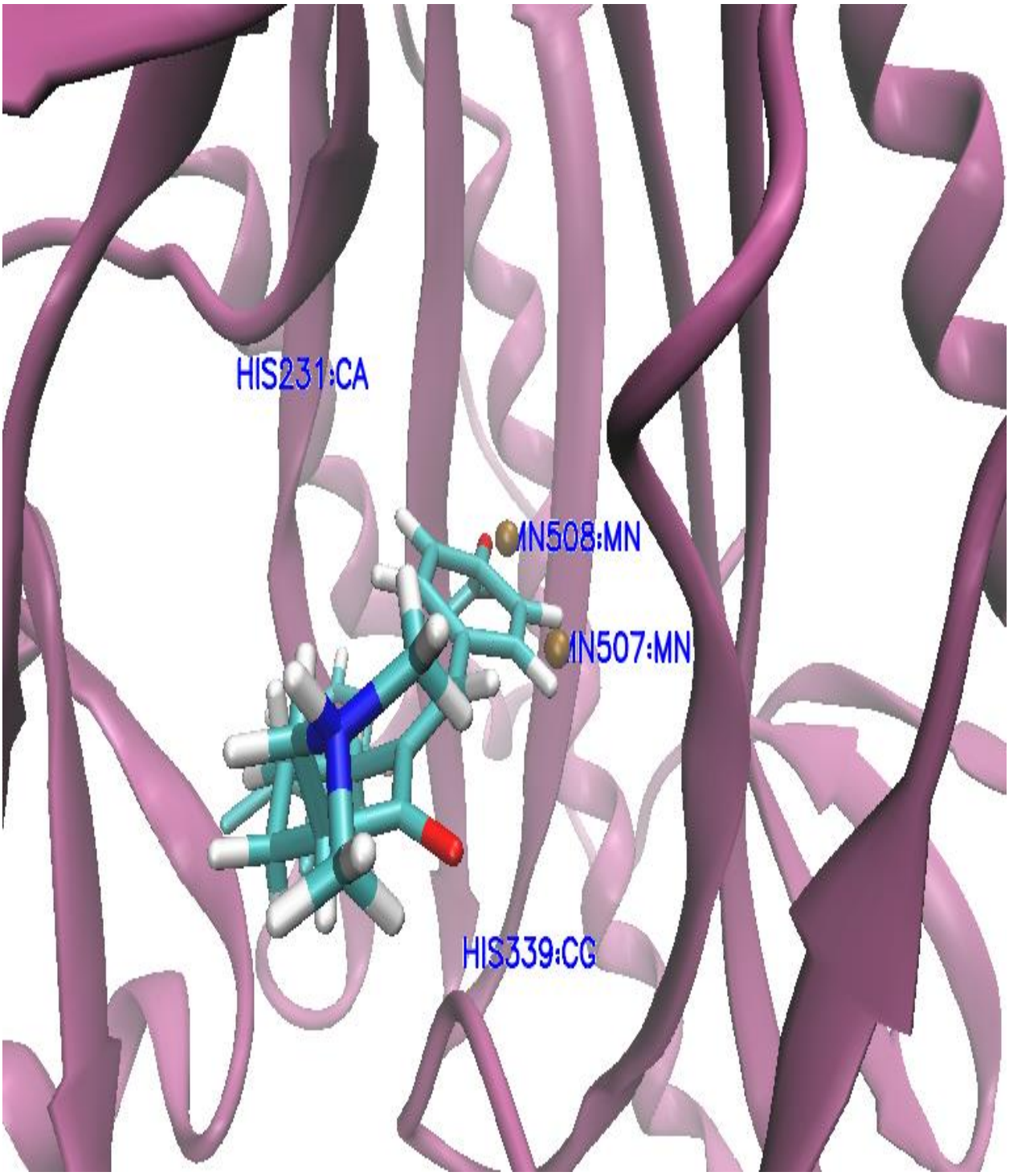

NC 1768

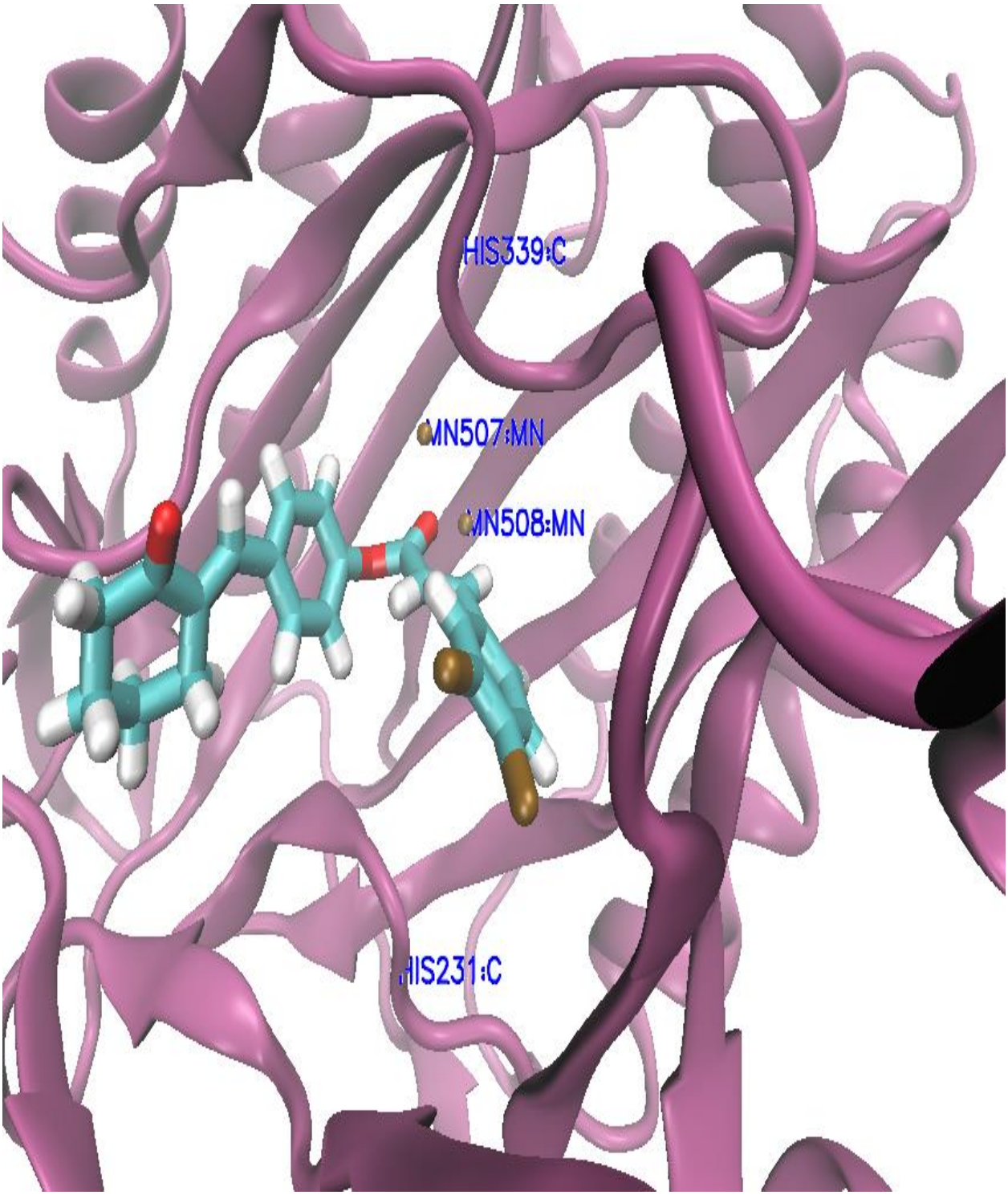

Figure 5.8: Docked view of NC 1773 and NC 1768 at the active site of MetAP2

5.5 Statistical analysis of correlation between cytotoxicity and physiochemical properties

Using the program IBM SPSS Statistics 26, the data for the 10 compounds in Table 5.1 and 5.2 with variables of HT29 IC_{50}, HCT116 IC_{50}, docking score, molecular weight (MW), LogP, and topological polar surface area (TPSA) were evaluated for correlations by Student's t-test for paired data. Statistical analysis was undertaken to find the correlation between the cytotoxicicity (IC_{50}) and different physicochemical properties. The bivariate linear models with logarithmic transformations that were taken for interpretation were linear model, linear-log model, and log-log model. The models were used for statistical significance using the Student's t-test for paired data. A $p<0.05$ was recorded as statistically significant. The results indicated that none of the parameters were significantly correlated with the cytotoxicity of the compounds. The complete result of the 3 models is given in Table 5.4. The data are expressed as the Pearson's correlation coefficient.

Table 5.4: Correlation between the cytotoxic properties

	Variables[a]			
Linear model	**DockingScore**	**TPSA**	**MW**	**LogP**
IC50_HT29	0.209	-0.020	0.165	0.033
IC50_HCT116	-0.197	-0.217	-0.125	0.056
Linear-Log model	**DockingScore**	**TPSA**	**MW**	**LogP**
LogIC50_HT29	-0.046	0.131	-0.085	-0.208
LogIC50_HCT116	0.252	0.056	-0.028	0.001
Log-Log model	**LogDockingScore**	**LogTPSA**	**LogMW**	**Log_LogP**
LogIC50_HT29	-0.043	0.139	-0.115	-0.203
LogIC50_HCT116	0.249	0.054	-0.064	-0.032

a The data are expressed as the Pearson's correlation coefficient with $p<0.05$ as the critical level of significance.

CHAPTER – 6

CONCLUSIONS

Colorectal cancer is one of the major causes of death worldwide. Designing of target-specific molecules has brought better success in developing new anticancer agents. In the present study we mainly focused on the investigation of curcumin analogs as novel anticancer molecules targeting the active site of MetAP2.

NC 2213, a drug design strategy by Pati *et. al.* to undertake structural modification of curcumin to produce novel synthetic analogs as anticancer agents demonstrated a significant decrease in MetAP2 expression, which was validated by western blot analysis.[78] The dienone pharmacophore was the alkylating active site where thiol could react with the electron-deficient olefinic carbon atom to cause the inhibition of the enzyme. This data suggested the importance of pursuing curcumin analogs as potential cytotoxic agents targeting MetAP2.

In the present study, 130 compounds were docked against MetAP2 enzyme and out of these the top 10 compounds that showed good results for their physicochemical properties assessment were taken for cytotoxic evaluation. Among the 10 compounds, 2 compounds (NC 1768 and NC 1773) had good IC_{50} profiles, and they were analyzed using a western blot. The western blot indicated that protein expression was reduced for NC 1773 against HT-29 cell line.

Once the validation procedures, protocols were in place, and the library of compounds was ready we were able to get the best compounds from their docking scores and the pharmacokinetic properties to be tried *in vitro* against HT-29, HCT-116, and CRL-1790 cells. After this, we were able to arrive at one compound, NC 1773 which showed *in silico* potential to be a very good MetAP2 inhibitor. The Student's t-test for paired data was not significant with $p>0.05$ in all 3 bivariate linear models. The result indicates that none of the parameters are critically involved in influencing neither the docking nor cytotoxicity or the bioactivity of the compounds. Therefore, there is no significant linear or non-linear relationship that exists between the independent and dependent variables as $p>0.05$.

The identification of novel MetAP2 inhibitors in colon cancer cells has provided new opportunities for preventive or therapeutic interventions by rational drug design. The compound NC 1773 has shown excellent results in docking and western blot analysis. Dunnett's post hoc test showed significance at $p<0.05$ for the treatment protocol of NC 1773 in comparison with control (cells with absence of treatment).

NC 1773 in comparison to NC 1768 had both desirable IC_{50} and GI_{50} values for it to be a better candidate in being a potent anticancer agent for the treatment of colon cancer. In comparison of the IC_{50} values against the non-malignant colon cells, compound 1768 showed to be highly cytotoxic to normal cells making compound 1773 as the compound of choice for further evaluations. Now, with the western blot analysis results, we can further strengthen the possibility of developing NC 1773 as a MetAP2 specific inhibitor, which may be therapeutically useful. It has an ideal IC_{50} profile and potential bioavailability which warrants further investigation for the mechanism of action of NC 1773. Further studies of this work may also reveal the mechanism of action of MetAP2 in colon carcinoma at large.

CHAPTER – 7

FUTURE SCOPE

NC 1773 and NC 1768 could be screened against MetAP2 recombinant protein to evaluate the MetAP2 inhibitory potential of these molecules. MetAP2 activity is determined by hydrolysis of methionine-*p*-nitroanilide as the substrate, as described in literature[15, 99, 100], methionine-*p*-nitroanilide would be hydrolyzed by MetAP2. The MetAP2 activity assay mixture (total volume of 500 µl) contains 50 mM Tris-HCl (pH 7.5), 0.25 mM methionine-*p*-nitroanilide as the substrate, and appropriate concentration of enzyme solution. The mixture would be incubated at 37 °C for 30 minutes and then left on ice for 15 minutes to terminate the enzyme reaction. Spectrophotometric determination of nitroanilide would be carried out at 405 nm. The amount that releases 1 µM/min *p*-nitroanilide would be taken as one unit of activity of aminopeptidase under the conditions set for assay. MetAP2 expression and activity would be evaluated using various concentrations of these compounds.

Several different analogs of NC 1773 and NC 1768 could be designed and synthesized for better anticancer activity and also see the impact of structural modification on activity. In the cases of NC 1773 and NC 1768 interactions with the receptor takes place at two points:

A) The two aryl rings and the amino acid residues
B) The ester keto group and the metal ions.

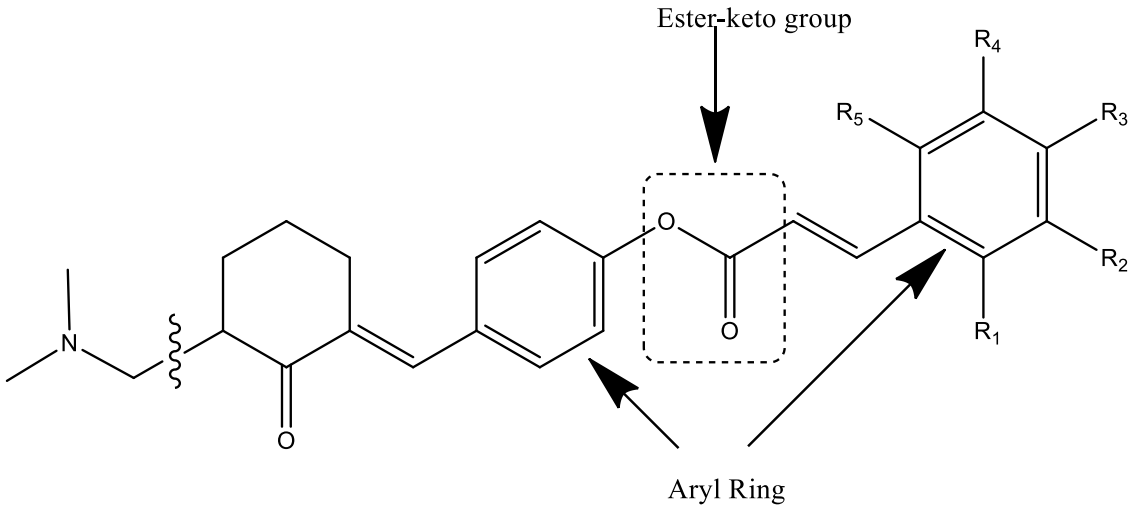

Some of the structural modifications could be as follows:

1. The first proposed modification will be the modification of the linker between both the aryl rings. Removal of unsaturated keto group of unsaturated ester portion of the linker to make the linker shorter. Only the –O– will be flanked by both the aryl rings. We will be able to understand whether the length of the linker has any impact or not on the potency of the drug towards MetAP2 inhibition. This will also give some idea of the importance of the distance between the aryl rings. The proposed structure is given below:

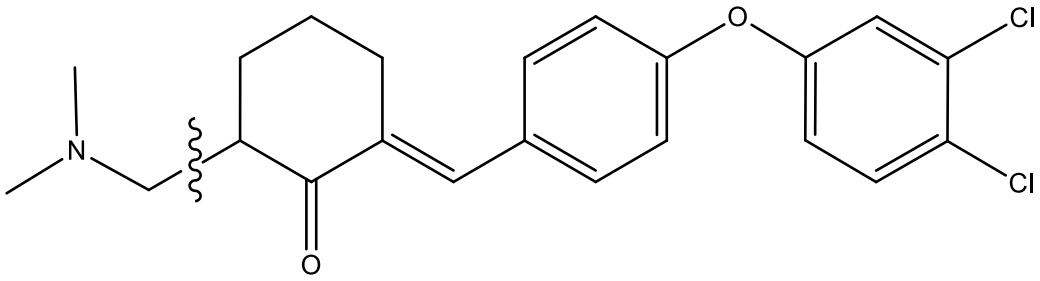

2. The second structural modification will be aimed to increase the size of the terminal aryl ring by the replacement of the terminal aryl ring with a naphthyl group. Th naphthyl ring is a natural choice due to its biological activities and to evaluate whether the bigger size of the terminal aryl ring has any impact on the drug activities. The proposed structure will be as follows:

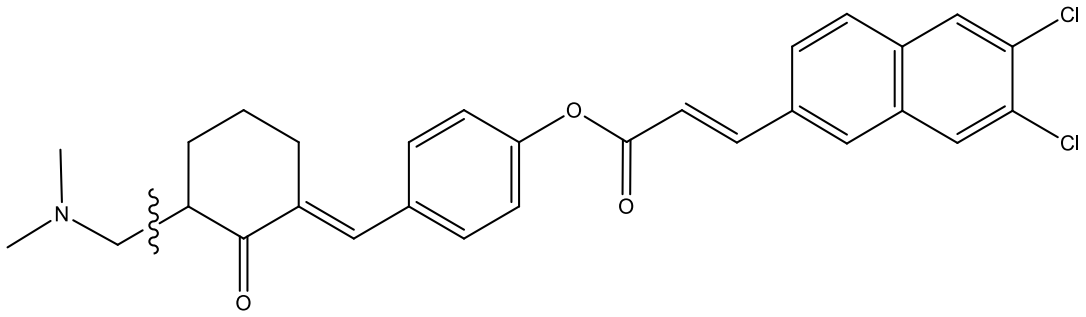

3. The third structural modification will be for the linker portion of the compound. Here we propose to change of linker from unsaturated keto-ester to an unsaturated thioester. Thioester functionality may increase the strength of the bonding to the manganese ions. The structure of the proposed analog is given below:

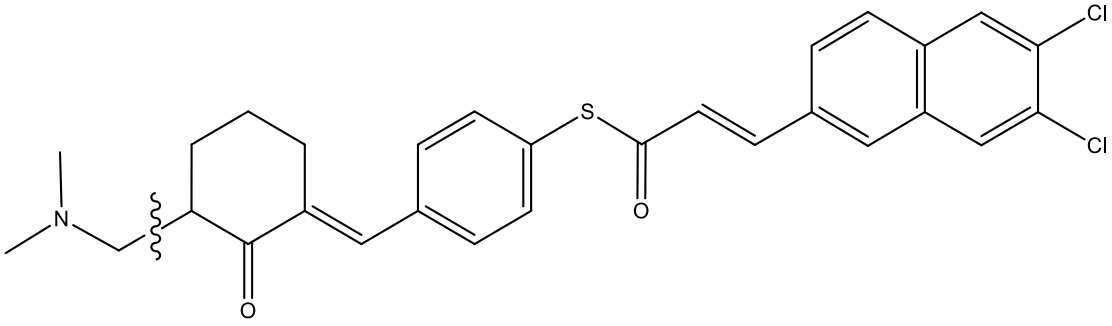

4. The fourth structural modification is around the substitution of Cl atoms in terminal aryl ring. The 3,4-dichloro substituents appear to the best among the aryl groups. We will synthesize compounds having different substitution patterns like 2,6-dichloro, and 3,5-dichloro substituents.

   In addition, 2,4,6-trichloro and 3,4,5-trichloro compounds can also be synthesized to see if increased biological activity is associated with the di-chloro substitution pattern; and whether the tri-chloro substitution is better than di-chloro substitution. The proposed structure as indicated below:

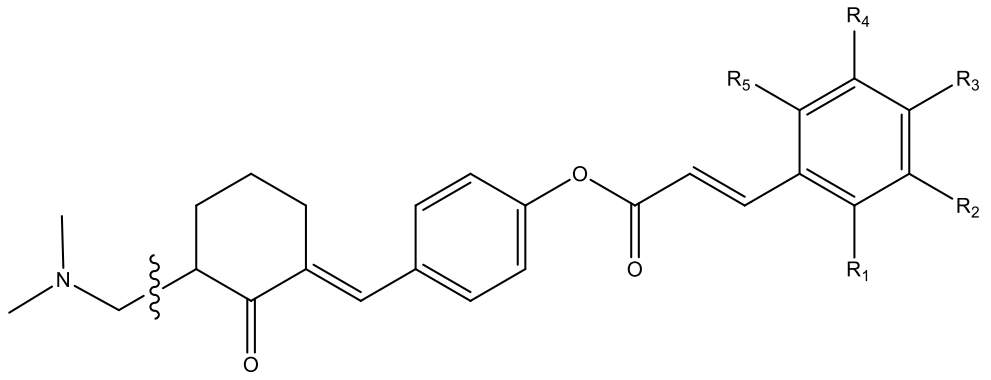

5. The fifth structural modification is also around the substitution of Cl atoms in the terminal aryl ring. The placement of bromo and iodo substituents in the terminal aryl ring should be considered to evaluate whether the size of the halogen group impacts the binding affinity and activity of the drug. The substitutions can be 3,4-dibromo; 3,4-diiodo; 2,6-dibromo; 2,6-diiodo; 3,5-dibromo and 3,5-diiodo. The proposed structure for the fourth modification given above can be used for this structural modification as well.

CHAPTER – 8

BIBLIOGRAPHY

1. Siegel, R. L.; Miller, K. D.; Goding Sauer, A.; Fedewa, S. A.; Butterly, L. F.; Anderson, J. C.; Cercek, A.; Smith, R. A.; Jemal, A. Colorectal cancer statistics, 2020. *CA Cancer J Clin* **2020,** 70, 145-164.
2. Selvakumar, P.; Lakshmikuttyamma, A.; Dimmock, J. R.; Sharma, R. K. Methionine aminopeptidase 2 and cancer. *Biochim Biophys Acta* **2006,** 1765, 148-54.
3. Giglione, C.; Boularot, A.; Meinnel, T. Protein N-terminal methionine excision. *Cell Mol Life Sci* **2004,** 61, 1455-74.
4. Jackson, R.; Hunter, T. Role of methionine in the initiation of haemoglobin synthesis. *Nature* **1970,** 227, 672-6.
5. Lowther, W. T.; Matthews, B. W. Structure and function of the methionine aminopeptidases. *Biochim Biophys Acta* **2000,** 1477, 157-67.
6. Lowther, W. T.; Zhang, Y.; Sampson, P. B.; Honek, J. F.; Matthews, B. W. Insights into the mechanism of Escherichia coli methionine aminopeptidase from the structural analysis of reaction products and phosphorus-based transition-state analogues. *Biochemistry* **1999,** 38, 14810-14819.
7. Bradshaw, R. A.; Brickey, W. W.; Walker, K. W. N-terminal processing: the methionine aminopeptidase and N alpha-acetyl transferase families. *Trends Biochem Sci* **1998,** 23, 263-7.
8. Hu, X.; Addlagatta, A.; Lu, J.; Matthews, B. W.; Liu, J. O. Elucidation of the function of type 1 human methionine aminopeptidase during cell cycle progression. *Proc Natl Acad Sci U S A* **2006,** 103, 18148-53.
9. Chiu, J.; Wong, J. W.; Hogg, P. J. Redox regulation of methionine aminopeptidase 2 activity. *J Biol Chem* **2014,** 289, 15035-43.
10. Xiao, Q.; Zhang, F.; Nacev, B. A.; Liu, J. O.; Pei, D. Protein N-terminal processing: substrate specificity of Escherichia coli and human methionine aminopeptidases. *Biochemistry* **2010,** 49, 5588-99.
11. Cellarier, E.; Durando, X.; Vasson, M.; Farges, M.; Demiden, A.; Maurizis, J.; Madelmont, J.; Chollet, P. Methionine dependency and cancer treatment. *Cancer treatment reviews* **2003,** 29, 489-499.
12. Mecham, J. O.; Rowitch, D.; Wallace, C. D.; Stern, P. H.; Hoffman, R. M. The metabolic defect of methionine dependence occurs frequently in human tumor cell lines. *Biochem Biophys Res Commun* **1983,** 117, 429-34.
13. Guo, H. Y.; Herrera, H.; Groce, A.; Hoffman, R. M. Expression of the biochemical defect of methionine dependence in fresh patient tumors in primary histoculture. *Cancer Res* **1993,** 53, 2479-83.

14. Kokkinakis, D. M.; Liu, X.; Chada, S.; Ahmed, M. M.; Shareef, M. M.; Singha, U. K.; Yang, S.; Luo, J. Modulation of gene expression in human central nervous system tumors under methionine deprivation-induced stress. *Cancer research* **2004,** 64, 7513-7525.
15. Selvakumar, P.; Lakshmikuttyamma, A.; Kanthan, R.; Kanthan, S. C.; Dimmock, J. R.; Sharma, R. K. High expression of methionine aminopeptidase 2 in human colorectal adenocarcinomas. *Clin Cancer Res* **2004,** 10, 2771-5.
16. Selvakumar, P.; Lakshmikuttyamma, A.; Lawman, Z.; Bonham, K.; Dimmock, J. R.; Sharma, R. K. Expression of methionine aminopeptidase 2, N-myristoyltransferase, and N-myristoyltransferase inhibitor protein 71 in HT29. *Biochem Biophys Res Commun* **2004,** 322, 1012-7.
17. Yin, S. Q.; Wang, J. J.; Zhang, C. M.; Liu, Z. P. The development of MetAP-2 inhibitors in cancer treatment. *Curr Med Chem* **2012,** 19, 1021-35.
18. Sheen, I. S.; Jeng, K. S.; Jeng, W. J.; Jeng, C. J.; Wang, Y. C.; Gu, S. L.; Tseng, S. Y.; Chu, C. M.; Lin, C. H.; Chang, K. M. Fumagillin treatment of hepatocellular carcinoma in rats: an in vivo study of antiangiogenesis. *World J Gastroenterol* **2005,** 11, 771-7.
19. Lowther, W. T.; Orville, A. M.; Madden, D. T.; Lim, S.; Rich, D. H.; Matthews, B. W. Escherichia coli methionine aminopeptidase: implications of crystallographic analyses of the native, mutant, and inhibited enzymes for the mechanism of catalysis. *Biochemistry* **1999,** 38, 7678-7688.
20. D'Souza V, M.; Holz, R. C. The methionyl aminopeptidase from Escherichia coli can function as an iron(II) enzyme. *Biochemistry* **1999,** 38, 11079-85.
21. Chang, Y. H.; Teichert, U.; Smith, J. A. Molecular cloning, sequencing, deletion, and overexpression of a methionine aminopeptidase gene from Saccharomyces cerevisiae. *J Biol Chem* **1992,** 267, 8007-11.
22. Ghosh, M.; Grunden, A. M.; Dunn, D. M.; Weiss, R.; Adams, M. W. Characterization of native and recombinant forms of an unusual cobalt-dependent proline dipeptidase (prolidase) from the hyperthermophilic archaeon Pyrococcus furiosus. *J Bacteriol* **1998,** 180, 4781-9.
23. Wang, J.; Sheppard, G. S.; Lou, P.; Kawai, M.; Park, C.; Egan, D. A.; Schneider, A.; Bouska, J.; Lesniewski, R.; Henkin, J. Physiologically relevant metal cofactor for methionine aminopeptidase-2 is manganese. *Biochemistry* **2003,** 42, 5035-42.
24. Leopoldini, M.; Russo, N.; Toscano, M. Which one among Zn(II), Co(II), Mn(II), and Fe(II) is the most efficient ion for the methionine aminopeptidase catalyzed reaction? *J Am Chem Soc* **2007,** 129, 7776-84.
25. Li, J. Y.; Cui, Y. M.; Chen, L. L.; Gu, M.; Li, J.; Nan, F. J.; Ye, Q. Z. Mutations at the S1 sites of methionine aminopeptidases from Escherichia coli and Homo sapiens reveal the residues critical for substrate specificity. *J Biol Chem* **2004,** 279, 21128-34.
26. Sin, N.; Meng, L.; Wang, M. Q.; Wen, J. J.; Bornmann, W. G.; Crews, C. M. The anti-angiogenic agent fumagillin covalently binds and inhibits the methionine aminopeptidase, MetAP-2. *Proc Natl Acad Sci U S A* **1997,** 94, 6099-103.

27. Ingber, D.; Fujita, T.; Kishimoto, S.; Sudo, K.; Kanamaru, T.; Brem, H.; Folkman, J. Synthetic analogues of fumagillin that inhibit angiogenesis and suppress tumour growth. *Nature* **1990,** 348, 555-7.
28. Kudelka, A. P.; Levy, T.; Verschraegen, C. F.; Edwards, C. L.; Piamsomboon, S.; Termrungruanglert, W.; Freedman, R. S.; Kaplan, A. L.; Kieback, D. G.; Meyers, C. A.; Jaeckle, K. A.; Loyer, E.; Steger, M.; Mante, R.; Mavligit, G.; Killian, A.; Tang, R. A phase I study of TNP-470 administered to patients with advanced squamous cell cancer of the cervix. *Clin Cancer Res* **1997,** 3, 1501-5.
29. Dezube, B. J.; Von Roenn, J. H.; Holden-Wiltse, J.; Cheung, T. W.; Remick, S. C.; Cooley, T. P.; Moore, J.; Sommadossi, J. P.; Shriver, S. L.; Suckow, C. W.; Gill, P. S. Fumagillin analog in the treatment of Kaposi's sarcoma: a phase I AIDS Clinical Trial Group study. AIDS Clinical Trial Group No. 215 Team. *J Clin Oncol* **1998,** 16, 1444-9.
30. Kruger, E. A.; Figg, W. D. TNP-470: an angiogenesis inhibitor in clinical development for cancer. *Expert Opin Investig Drugs* **2000,** 9, 1383-96.
31. Jia, L.; Zhang, M. H.; Yuan, S. Z.; Huang, W. G. Antiangiogenic therapy for human pancreatic carcinoma xenografts in nude mice. *World J Gastroenterol* **2005,** 11, 447-50.
32. Kidoikhammouan, S.; Seubwai, W.; Silsirivanit, A.; Wongkham, S.; Sawanyawisuth, K.; Wongkham, C. Blocking of methionine aminopeptidase-2 by TNP-470 induces apoptosis and increases chemosensitivity of cholangiocarcinoma. *J Cancer Res Ther* **2019,** 15, 148-152.
33. Kidoikhammouan, S.; Seubwai, W.; Tantapotinan, N.; Silsirivanit, A.; Wongkham, S.; Sawanyawisuth, K.; Wongkham, C. TNP-470, a methionine aminopeptidase-2 inhibitor, inhibits cell proliferation, migration and invasion of human cholangiocarcinoma cells in vitro. *Asian Pac J Cancer Prev* **2012,** 13 Suppl, 155-60.
34. Chun, E.; Han, C. K.; Yoon, J. H.; Sim, T. B.; Kim, Y. K.; Lee, K. Y. Novel inhibitors targeted to methionine aminopeptidase 2 (MetAP2) strongly inhibit the growth of cancers in xenografted nude model. *Int J Cancer* **2005,** 114, 124-30.
35. S.-Q. Yin, J.-J. W., C.-M. Zhang, Z.-P. Liu. The Development of MetAP-2 Inhibitors in Cancer Treatment. *Current Medicinal Chemistry* **2012,** 19, 1021 - 1035.
36. Heinrich, T.; Seenisamy, J.; Becker, F.; Blume, B.; Bomke, J.; Dietz, M.; Eckert, U.; Friese-Hamim, M.; Gunera, J.; Hansen, K.; Leuthner, B.; Musil, D.; Pfalzgraf, J.; Rohdich, F.; Siegl, C.; Spuck, D.; Wegener, A.; Zenke, F. T. Identification of Methionine Aminopeptidase-2 (MetAP-2) Inhibitor M8891: A Clinical Compound for the Treatment of Cancer. *J Med Chem* **2019,** 62, 11119-11134.
37. Friese-Hamim, M.; Bogatyrova, O.; Ortiz, M. J.; Wienke, D.; Heinrich, T.; Rohdich, F.; Duecker, K.; Schultes, C.; Huck, B.; Zenke, F. T.; Blaukat, A. Abstract 3075: Antitumor activity of M8891, a potent and reversible inhibitor of methionine aminopeptidase 2. *Cancer Research* **2019,** 79, 3075-3075.
38. McBride, C.; Cheruvallath, Z.; Komandla, M.; Tang, M.; Farrell, P.; Lawson, J. D.; Vanderpool, D.; Wu, Y.; Dougan, D. R.; Plonowski, A.; Holub, C.; Larson, C. Discovery of

potent, reversible MetAP2 inhibitors via fragment based drug discovery and structure based drug design-Part 2. *Bioorg Med Chem Lett* **2016,** 26, 2779-2783.

39. Cheruvallath, Z.; Tang, M.; McBride, C.; Komandla, M.; Miura, J.; Ton-Nu, T.; Erikson, P.; Feng, J.; Farrell, P.; Lawson, J. D.; Vanderpool, D.; Wu, Y.; Dougan, D. R.; Plonowski, A.; Holub, C.; Larson, C. Discovery of potent, reversible MetAP2 inhibitors via fragment based drug discovery and structure based drug design-Part 1. *Bioorg Med Chem Lett* **2016,** 26, 2774-2778.
40. Marino, J. P., Jr.; Fisher, P. W.; Hofmann, G. A.; Kirkpatrick, R. B.; Janson, C. A.; Johnson, R. K.; Ma, C.; Mattern, M.; Meek, T. D.; Ryan, M. D.; Schulz, C.; Smith, W. W.; Tew, D. G.; Tomazek, T. A., Jr.; Veber, D. F.; Xiong, W. C.; Yamamoto, Y.; Yamashita, K.; Yang, G.; Thompson, S. K. Highly potent inhibitors of methionine aminopeptidase-2 based on a 1,2,4-triazole pharmacophore. *J Med Chem* **2007,** 50, 3777-85.
41. Kallander, L. S.; Lu, Q.; Chen, W.; Tomaszek, T.; Yang, G.; Tew, D.; Meek, T. D.; Hofmann, G. A.; Schulz-Pritchard, C. K.; Smith, W. W.; Janson, C. A.; Ryan, M. D.; Zhang, G. F.; Johanson, K. O.; Kirkpatrick, R. B.; Ho, T. F.; Fisher, P. W.; Mattern, M. R.; Johnson, R. K.; Hansbury, M. J.; Winkler, J. D.; Ward, K. W.; Veber, D. F.; Thompson, S. K. 4-Aryl-1,2,3-triazole: a novel template for a reversible methionine aminopeptidase 2 inhibitor, optimized to inhibit angiogenesis in vivo. *J Med Chem* **2005,** 48, 5644-7.
42. Xu, W.; Lu, J. P.; Ye, Q. Z. Structural analysis of bengamide derivatives as inhibitors of methionine aminopeptidases. *J Med Chem* **2012,** 55, 8021-7.
43. Morgen, M.; Jost, C.; Malz, M.; Janowski, R.; Niessing, D.; Klein, C. D.; Gunkel, N.; Miller, A. K. Spiroepoxytriazoles Are Fumagillin-like Irreversible Inhibitors of MetAP2 with Potent Cellular Activity. *ACS Chem Biol* **2016,** 11, 1001-11.
44. Pillalamarri, V.; Arya, T.; Haque, N.; Bala, S. C.; Marapaka, A. K.; Addlagatta, A. Discovery of natural product ovalicin sensitive type 1 methionine aminopeptidases: molecular and structural basis. *Biochem J* **2019,** 476, 991-1003.
45. Heinrich, T.; Buchstaller, H. P.; Cezanne, B.; Rohdich, F.; Bomke, J.; Friese-Hamim, M.; Krier, M.; Knochel, T.; Musil, D.; Leuthner, B.; Zenke, F. Novel reversible methionine aminopeptidase-2 (MetAP-2) inhibitors based on purine and related bicyclic templates. *Bioorg Med Chem Lett* **2017,** 27, 551-556.
46. Heinrich, T.; Seenisamy, J.; Blume, B.; Bomke, J.; Calderini, M.; Eckert, U.; Friese-Hamim, M.; Kohl, R.; Lehmann, M.; Leuthner, B.; Musil, D.; Rohdich, F.; Zenke, F. T. Discovery and Structure-Based Optimization of Next-Generation Reversible Methionine Aminopeptidase-2 (MetAP-2) Inhibitors. *J Med Chem* **2019,** 62, 5025-5039.
47. Brouet, I.; Ohshima, H. Curcumin, an anti-tumour promoter and anti-inflammatory agent, inhibits induction of nitric oxide synthase in activated macrophages. *Biochem Biophys Res Commun* **1995,** 206, 533-40.
48. Dikshit, M.; Rastogi, L.; Shukla, R.; Srimal, R. C. Prevention of ischaemia-induced biochemical changes by curcumin & quinidine in the cat heart. *Indian J Med Res* **1995,** 101, 31-5.

49. Lestari, M. L.; Indrayanto, G. Curcumin. *Profiles Drug Subst Excip Relat Methodol* **2014,** 39, 113-204.
50. Mahady, G. B.; Pendland, S. L.; Yun, G.; Lu, Z. Z. Turmeric (Curcuma longa) and curcumin inhibit the growth of Helicobacter pylori, a group 1 carcinogen. *Anticancer Res* **2002,** 22, 4179-81.
51. Berger, A. L.; Randak, C. O.; Ostedgaard, L. S.; Karp, P. H.; Vermeer, D. W.; Welsh, M. J. Curcumin stimulates cystic fibrosis transmembrane conductance regulator Cl- channel activity. *J Biol Chem* **2005,** 280, 5221-6.
52. Vera-Ramirez, L.; Perez-Lopez, P.; Varela-Lopez, A.; Ramirez-Tortosa, M.; Battino, M.; Quiles, J. L. Curcumin and liver disease. *Biofactors* **2013,** 39, 88-100.
53. Wright, L. E.; Frye, J. B.; Gorti, B.; Timmermann, B. N.; Funk, J. L. Bioactivity of turmeric-derived curcuminoids and related metabolites in breast cancer. *Curr Pharm Des* **2013,** 19, 6218-25.
54. Prasad, S.; Gupta, S. C.; Tyagi, A. K.; Aggarwal, B. B. Curcumin, a component of golden spice: From bedside to bench and back. *Biotechnol. Adv.* 32, 1053–1064.
55. Bisht, S.; Schlesinger, M.; Rupp, A.; Schubert, R.; Nolting, J.; Wenzel, J.; Holdenrieder, S.; Brossart, P.; Bendas, G.; Feldmann, G. A liposomal formulation of the synthetic curcumin analog EF24 (Lipo-EF24) inhibits pancreatic cancer progression: towards future combination therapies. *J Nanobiotechnology* **2016,** 14, 57.
56. Mimeault, M.; Batra, S. K. Potential applications of curcumin and its novel synthetic analogs and nanotechnology-based formulations in cancer prevention and therapy. *Chin Med* **2011,** 6, 31.
57. Bill, M. A.; Nicholas, C.; Mace, T. A.; Etter, J. P.; Li, C.; Schwartz, E. B.; Fuchs, J. R.; Young, G. S.; Lin, L.; Lin, J.; He, L.; Phelps, M.; Li, P. K.; Lesinski, G. B. Structurally modified curcumin analogs inhibit STAT3 phosphorylation and promote apoptosis of human renal cell carcinoma and melanoma cell lines. *PLoS One* **2012,** 7, e40724.
58. Bandgar, B. P.; Hote, B. S.; Jalde, S. S.; Gacche, R. N. Synthesis and biological evaluation of novel curcumin analogues as anti-inflammatory, anti-cancer and anti-oxidant agents. *Medicinal Chemistry Research* **2012,** 21, 3006-3014.
59. Bandgar, B. P.; Kinkar, S. N.; Chavan, H. V.; Jalde, S. S.; Shaikh, R. U.; Gacche, R. N. Synthesis and biological evaluation of asymmetric indole curcumin analogs as potential anti-inflammatory and antioxidant agents. *J Enzyme Inhib Med Chem* **2014,** 29, 7-11.
60. Campos, C. A.; Gianino, J. B.; Bailey, B. J.; Baluyut, M. E.; Wiek, C.; Hanenberg, H.; Shannon, H. E.; Pollok, K. E.; Ashfeld, B. L. Design, synthesis, and evaluation of curcumin-derived arylheptanoids for glioblastoma and neuroblastoma cytotoxicity. *Bioorg Med Chem Lett* **2013,** 23, 6874-8.
61. Chaudhary, M.; Kumar, N.; Baldi, A.; Chandra, R.; Babu, M. A.; Madan, J. 4-Bromo-4'-chloro pyrazoline analog of curcumin augmented anticancer activity against human cervical cancer, HeLa cells: in silico-guided analysis, synthesis, and in vitro cytotoxicity. *J Biomol Struct Dyn* **2020,** 38, 1335-1353.

62. Zuo, Y.; Yu, Y.; Wang, S.; Shao, W.; Zhou, B.; Lin, L.; Luo, Z.; Huang, R.; Du, J.; Bu, X. Synthesis and cytotoxicity evaluation of biaryl-based chalcones and their potential in TNFalpha-induced nuclear factor-kappaB activation inhibition. *Eur J Med Chem* **2012,** 50, 393-404.
63. Liang, B.; Liu, Z.; Cao, Y.; Zhu, C.; Zuo, Y.; Huang, L.; Wen, G.; Shang, N.; Chen, Y.; Yue, X.; Du, J.; Li, B.; Zhou, B.; Bu, X. MC37, a new mono-carbonyl curcumin analog, induces G2/M cell cycle arrest and mitochondria-mediated apoptosis in human colorectal cancer cells. *Eur J Pharmacol* **2017,** 796, 139-148.
64. Anto, R. J.; Kuttan, G.; Babu, K. V. D.; Rajasekharan, K. N.; Kuttan, R. Anti-tumour and free radical scavenging activity of synthetic curcuminoids. *Int. J. Pharm.* **1996,** 131, 1-7.
65. Fuchs, J. R.; Pandit, B.; Bhasin, D.; Etter, J. P.; Regan, N.; Abdelhamid, D.; Li, C.; Lin, J.; Li, P.-K. Structure-activity relationship studies of curcumin analogues. *Bioorg. Med. Chem. Lett.* **2009,** 19, 2065–2069.
66. Simoni, D.; Rizzi, M.; Rondanin, R.; Baruchello, R.; Marchetti, P.; Invidiata, F. P.; Labbozzetta, M.; Poma, P.; Carina, V.; Notarbartolo, M.; al., e. Antitumor effects of curcumin and structurally β-diketone modified analogs on multidrug resistant cancer cells. *Bioorg. Med. Chem. Lett.* **2008,** 18, 845-849.
67. Pae, H.-O.; Jeong, S.-O.; Kim, H. S.; Kim, S. H.; Song, Y. S.; Kim, S.-K.; Chai, K.-Y.; Chung, H.-T. Dimethoxycurcumin, a synthetic curcumin analogue with higher metabolic stability, inhibits NO production, inducible NO synthase expression and NF-κB activation in RAW264.7 macrophages activated with LPS. *Mol. Nutr. Food Res.* **2008,** 52, 1082–1091.
68. Pati, H. N.; Das, U.; Sharma, R. K.; Dimmock, J. R. Cytotoxic thiol alkylators. *Mini Reviews in Medicinal Chemistry* **2007,** 7, 131-139.
69. Dimmock, J.; Sidhu, K.; Chen, M.; Reid, R.; Allen, T.; Kao, G.; Truitt, G. Evaluation of some Mannich bases of cycloalkanones and related compounds for cytotoxic activity. *European journal of medicinal chemistry* **1993,** 28, 313-322.
70. Das, U.; Sakagami, H.; Chu, Q.; Wang, Q.; Kawase, M.; Selvakumar, P.; Sharma, R. K.; Dimmock, J. R. 3,5-Bis(benzylidene)-1-[4-2-(morpholin-4-yl)ethoxyphenylcarbonyl]-4-piperidone hydrochloride: a lead tumor-specific cytotoxin which induces apoptosis and autophagy. *Bioorg Med Chem Lett* **2010,** 20, 912-7.
71. Jha, A.; Dimmock, J. R. Syntheses of 4-(3,5-Bisphenylmethylene-4-oxo-piperidin-1-yl)-4-oxo-but-2 Z -enoic Acid Arylamides as Candidate Cytotoxic Agents. *Synthetic Communications* **2003,** 33, 1211-1223.
72. Jha, A.; Duffield, K. M.; Ness, M. R.; Ravoori, S.; Andrews, G.; Bhullar, K. S.; Rupasinghe, H. P.; Balzarini, J. Curcumin-inspired cytotoxic 3,5-bis(arylmethylene)-1-(N-(ortho-substituted aryl)maleamoyl)-4-piperidones: A novel group of topoisomerase II alpha inhibitors. *Bioorg Med Chem* **2015,** 23, 6404-17.
73. Ocasio-Malave, C.; Donate, M. J.; Sanchez, M. M.; Sosa-Rivera, J. M.; Mooney, J. W.; Pereles-De Leon, T. A.; Carballeira, N. M.; Zayas, B.; Velez-Gerena, C. E.; Martinez-Ferrer, M.; Sanabria-Rios, D. J. Synthesis of novel 4-Boc-piperidone chalcones and evaluation of

their cytotoxic activity against highly-metastatic cancer cells. *Bioorg Med Chem Lett* **2020,** 30, 126760.

74. Dimmock, J. R.; Padmanilayam, M. P.; Puthucode, R. N.; Nazarali, A. J.; Motaganahalli, N. L.; Zello, G. A.; Quail, J. W.; Oloo, E. O.; Kraatz, H. B.; Prisciak, J. S.; Allen, T. M.; Santos, C. L.; Balzarini, J.; De Clercq, E.; Manavathu, E. K. A conformational and structure-activity relationship study of cytotoxic 3,5-bis(arylidene)-4-piperidones and related N-acryloyl analogues. *J Med Chem* **2001,** 44, 586-93.
75. Das, U.; Pati, H. N.; Sakagami, H.; Hashimoto, K.; Kawase, M.; Balzarini, J.; De Clercq, E.; Dimmock, J. R. 3,5-Bis(benzylidene)-1-[3-(2-hydroxyethylthio)propanoyl]piperidin-4-ones: a novel cluster of potent tumor-selective cytotoxins. *J Med Chem* **2011,** 54, 3445-9.
76. Das, U.; Alcorn, J.; Shrivastav, A.; Sharma, R. K.; De Clercq, E.; Balzarini, J.; Dimmock, J. R. Design, synthesis and cytotoxic properties of novel 1-[4-(2-alkylaminoethoxy)phenylcarbonyl]-3,5-bis(arylidene)-4-piperidones and related compounds. *Eur J Med Chem* **2007,** 42, 71-80.
77. Das, U.; Sharma, R. K.; Dimmock, J. R. 1,5-diaryl-3-oxo-1,4-pentadienes: a case for antineoplastics with multiple targets. *Curr Med Chem* **2009,** 16, 2001-20.
78. Pati, H. N.; Das, U.; Quail, J. W.; Kawase, M.; Sakagami, H.; Dimmock, J. R. Cytotoxic 3,5-bis(benzylidene)piperidin-4-ones and N-acyl analogs displaying selective toxicity for malignant cells. *Eur J Med Chem* **2008,** 43, 1-7.
79. Selvakumar, P.; Lakshmikuttyamma, A.; Das, U.; Pati, H. N.; Dimmock, J. R.; Sharma, R. K. NC2213: a novel methionine aminopeptidase 2 inhibitor in human colon cancer HT29 cells. *Mol Cancer* **2009,** 8, 65.
80. Guedes, I. A.; de Magalhaes, C. S.; Dardenne, L. E. Receptor-ligand molecular docking. *Biophys Rev* **2014,** 6, 75-87.
81. Lipinski, C. A.; Lombardo, F.; Dominy, B. W.; Feeney, P. J. Experimental and computational approaches to estimate solubility and permeability in drug discovery and development settings. *Advanced drug delivery reviews* **1997,** 23, 3-25.
82. *SciFinder*. American Chemical Society: [Columbus, Ohio], 2007.
83. *PubMed*. National Library of Medicine: [Bethesda, Md.], 1996.
84. Friesner, R. A.; Banks, J. L.; Murphy, R. B.; Halgren, T. A.; Klicic, J. J.; Mainz, D. T.; Repasky, M. P.; Knoll, E. H.; Shelley, M.; Perry, J. K. Glide: a new approach for rapid, accurate docking and scoring. 1. Method and assessment of docking accuracy. *Journal of medicinal chemistry* **2004,** 47, 1739-1749.
85. Sastry, G. M.; Adzhigirey, M.; Day, T.; Annabhimoju, R.; Sherman, W. Protein and ligand preparation: parameters, protocols, and influence on virtual screening enrichments. *J Comput Aided Mol Des* **2013,** 27, 221-34.
86. Sherman, W.; Day, T.; Jacobson, M. P.; Friesner, R. A.; Farid, R. Novel procedure for modeling ligand/receptor induced fit effects. *J Med Chem* **2006,** 49, 534-53.

87. Daina, A.; Michielin, O.; Zoete, V. SwissADME: a free web tool to evaluate pharmacokinetics, drug-likeness and medicinal chemistry friendliness of small molecules. *Sci Rep* **2017,** 7, 42717.
88. Members, S. I. B. S. I. o. B. The SIB Swiss Institute of Bioinformatics' resources: focus on curated databases. *Nucleic Acids Res* **2016,** 44, D27-37.
89. Skehan, P.; Storeng, R.; Scudiero, D.; Monks, A.; McMahon, J.; Vistica, D.; Warren, J. T.; Bokesch, H.; Kenney, S.; Boyd, M. R. New colorimetric cytotoxicity assay for anticancer-drug screening. *J Natl Cancer Inst* **1990,** 82, 1107-12.
90. Park, J.; Meisler, A.; Cartwright, C. c-Yes tyrosine kinase activity in human colon carcinoma. *Oncogene* **1993,** 8, 2627.
91. MM., B. A rapid and sensitive method for the quantification of microgram quantities of protein utilizing the priniciple of protein-dye binding. *Anal Biochem* **1976,** 72, 248-54.
92. UK., L. Cleavage of structural proteins during the assembly of the head of bacteriophage T4. *Nature (Lond)* **1970,** 227, 680-5.
93. Towbin, H.; Staehelin, T.; Gordon, J. Electrophoretic transfer of proteins from polyacrylamide gels to nitrocellulose sheets: procedure and some applications. *Proc Natl Acad Sci U S A* **1979,** 76, 4350-4.
94. Kar, P.; Agnihotri, S. K.; Sharma, A.; Sachan, R.; Lal Bhatt, M.; Sachdev, M. A protocol for stripping and reprobing of Western blots originally developed with colorimetric substrate TMB. *Electrophoresis* **2012,** 33, 3062-5.
95. Corp, I. Ibm SPSS statistics: version 23. In Author Armonk, NY: 2016.
96. Shaikh, S. K. J.; Kamble, R. R.; Bayannavar, P. K.; Somagond, S. M.; Joshi, S. D. Triazolothiadizepinylquinolines as potential MetAP-2 and NMT inhibitors: Microwave-assisted synthesis, pharmacological evaluation and molecular docking studies. *Journal of Molecular Structure* **2020,** 1203, 127445.
97. Chen, C.-K.; Doyle, P. S.; Yermalitskaya, L. V.; Mackey, Z. B.; Ang, K. K. H.; McKerrow, J. H.; Podust, L. M. Trypanosoma cruzi CYP51 inhibitor derived from a Mycobacterium tuberculosis screen hit. *PLoS Negl Trop Dis* **2009,** 3, e372-e372.
98. Boyd, M.; Paull, K. Some practical considerations and applications of the national cancer institute in vitro anticancer drug discovery screen. *Drug Development Research* **1995,** 34.
99. Nirasawa S, N. Y., Zhang ZZ, Yoshida M, Hayashi K. Intramolecular chaperone and inhibitor activities of a propeptide from a bacterial zinc aminopeptidase. *Biochem J.* **1999,** 341, 25-31.
100. Izawa, N.; Ishikawa, S.; Tanokura, T.; Ohta, K.; Hayashi, K. Purification and characterization of Aeromonas caviae aminopeptidase possessing debittering activity. *Journal of Agricultural and Food Chemistry* **1997,** 45, 4897-4902.

****